Revealing the environment of a supermassive black hole

Pierre-Olivier Petrucci
Institut de Planetologie et d'Astrophysique de Grenoble

In collaboration with

Jelle Kaastra, Nahum Arav, Ehud Behar, Stefano Bianchi, Josh Bloom, Alex Blustin, Graziella Branduardi-Raymont, Massimo Cappi, Elisa Costantini, Mauro Dadina, Rob Detmers, Jacobo Ebrero, Peter Jonker, Chris Klein, Jerry Kriss, Piotr Lubinski, Julien Malzac, Missagh Mehdipour, Stéphane Paltani, Ciro Pinto, Gabriele Ponti, Eva Ratti, Katrien Steenbrugge, Cor de Vries

Outline

- Active Galactic Nuclei:
  - Main generalities
  - The Big picture
- The case of Mrk 509
  - Origin of the High energy emission
  - Warm absorber and Outflows

Active Galactic NUCLEI (AGN) Zoology

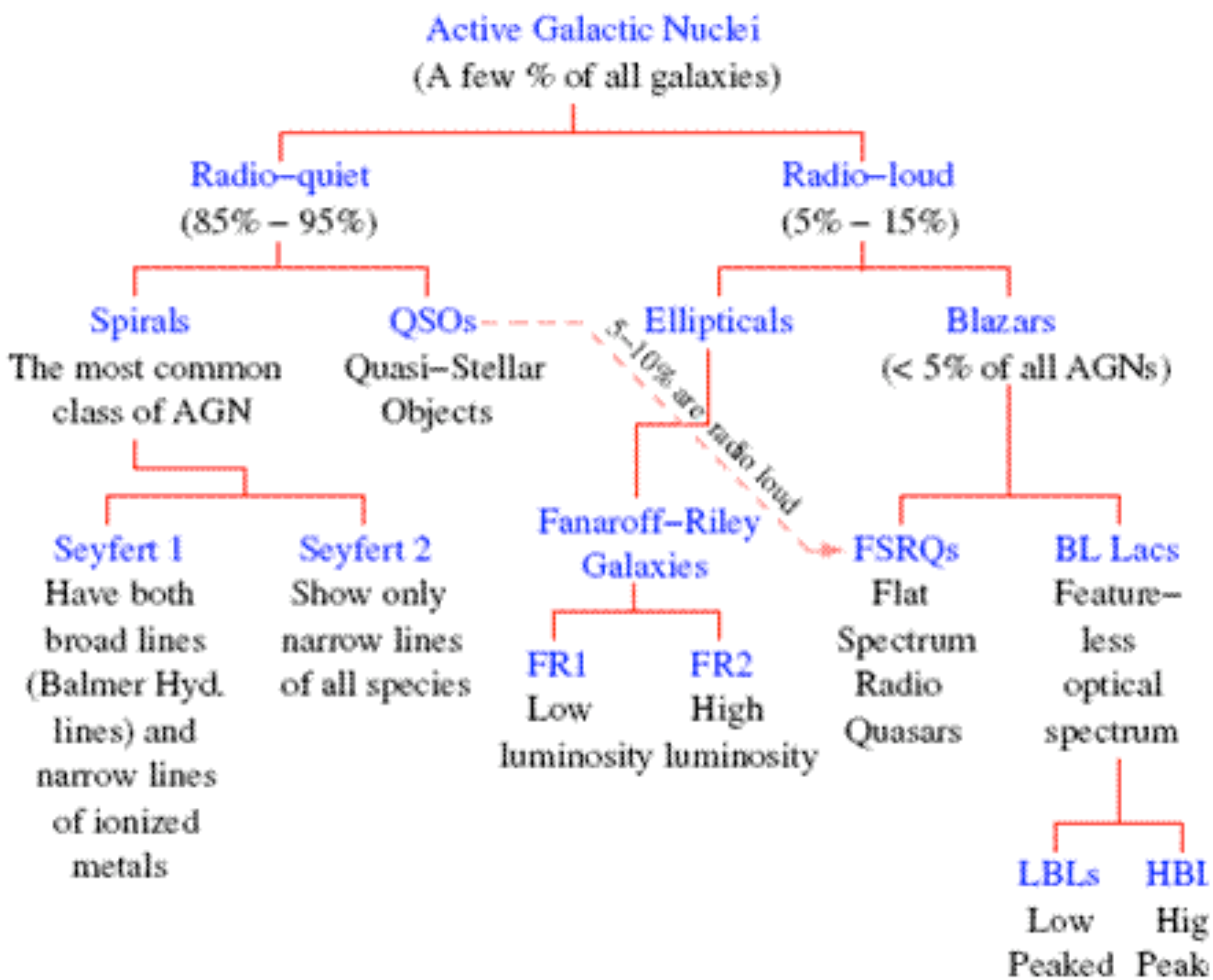

Active Galactic NUCLEI (AGN) Zoology

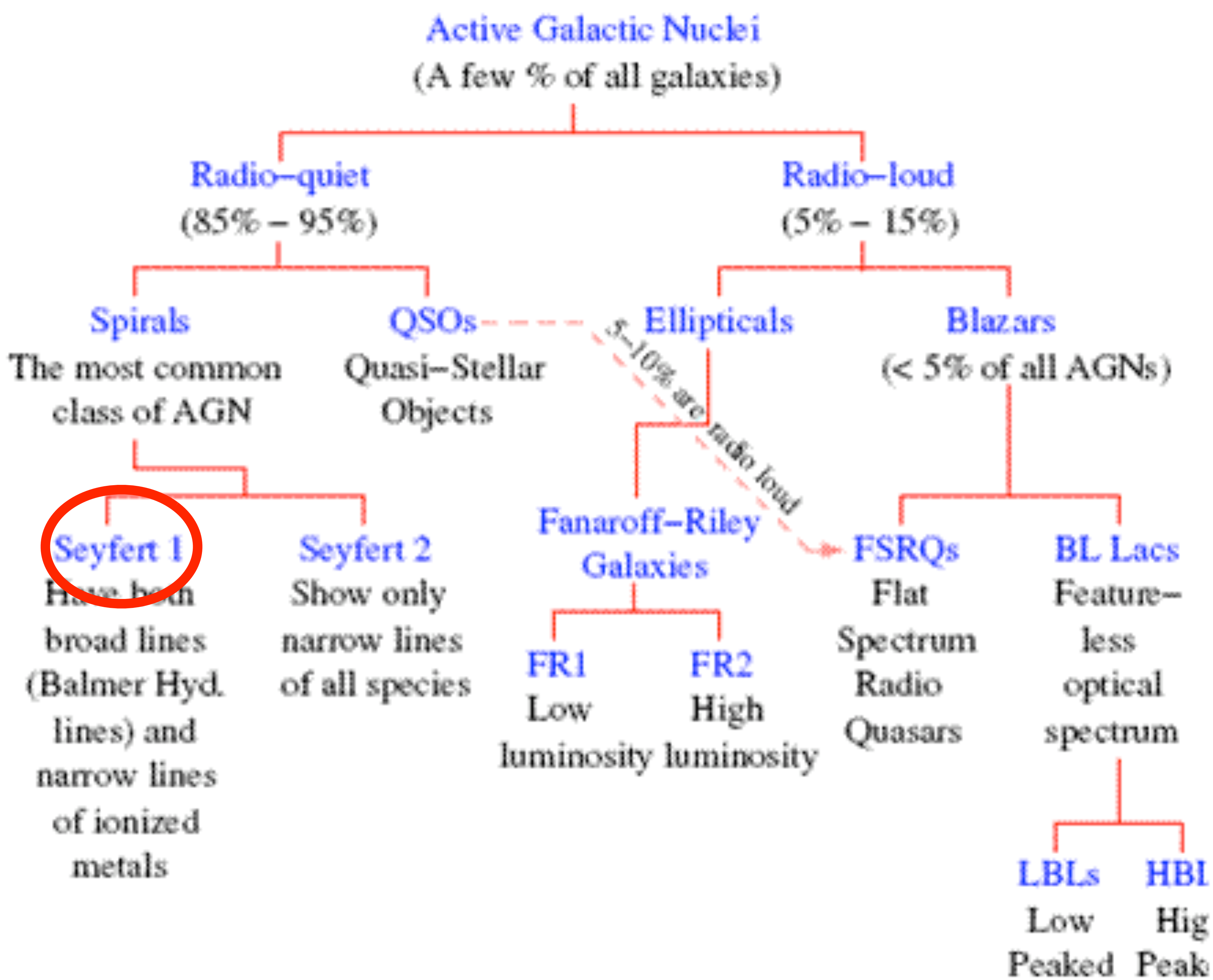

The AGN Environment

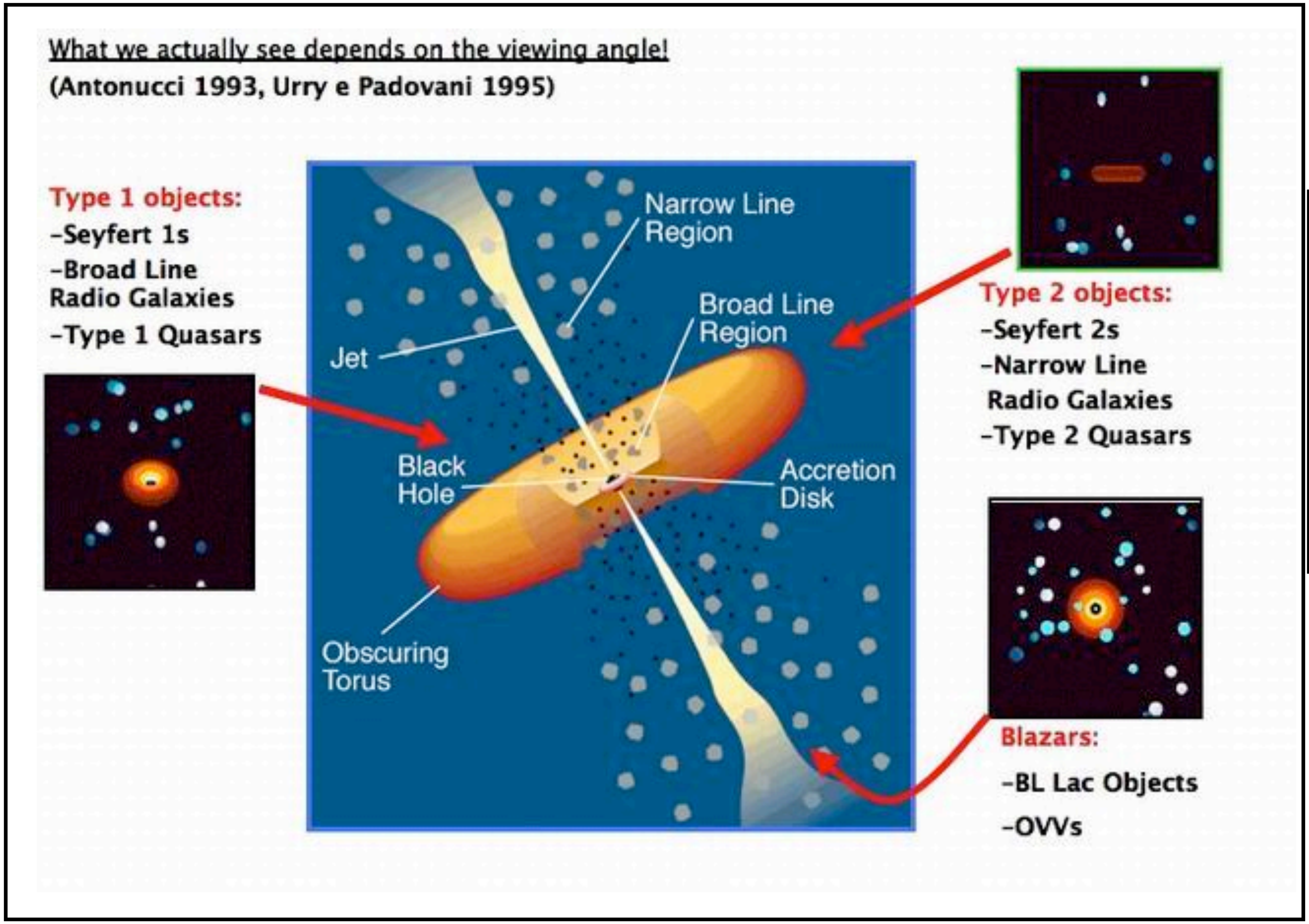

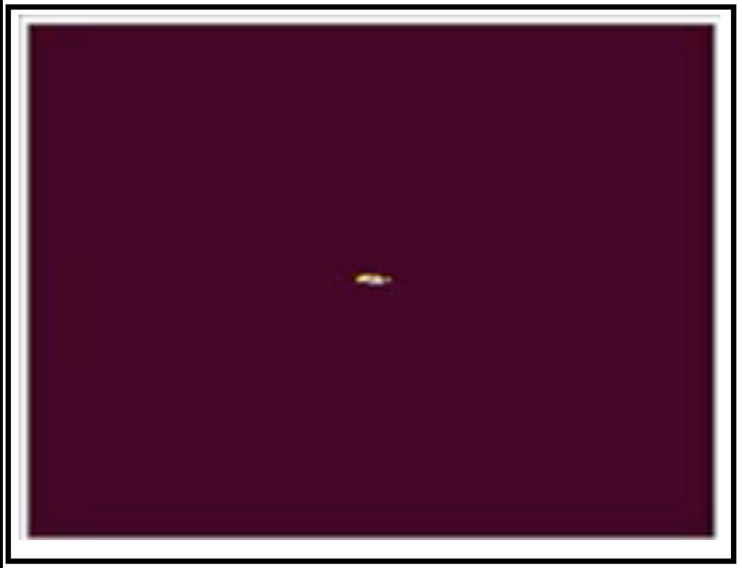

BroadBand Emission

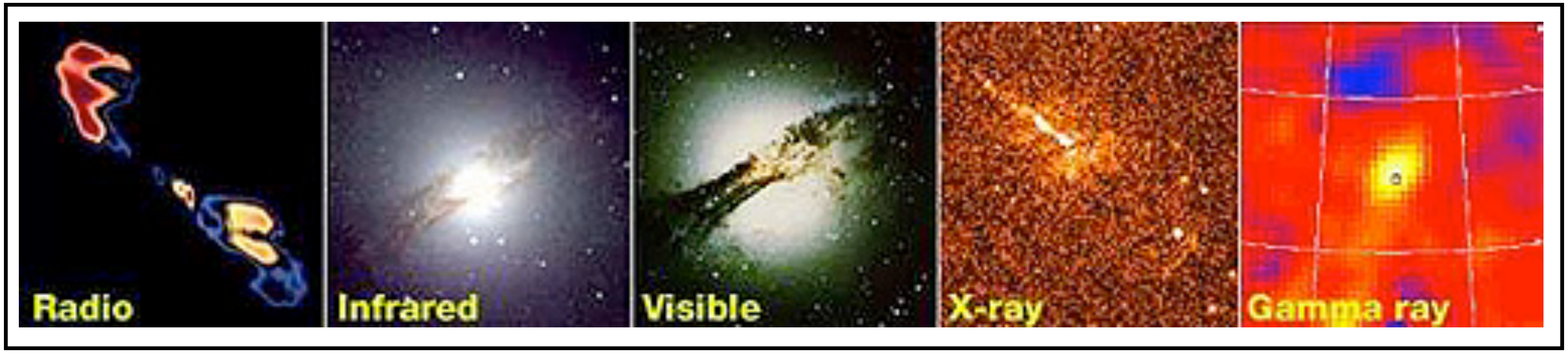

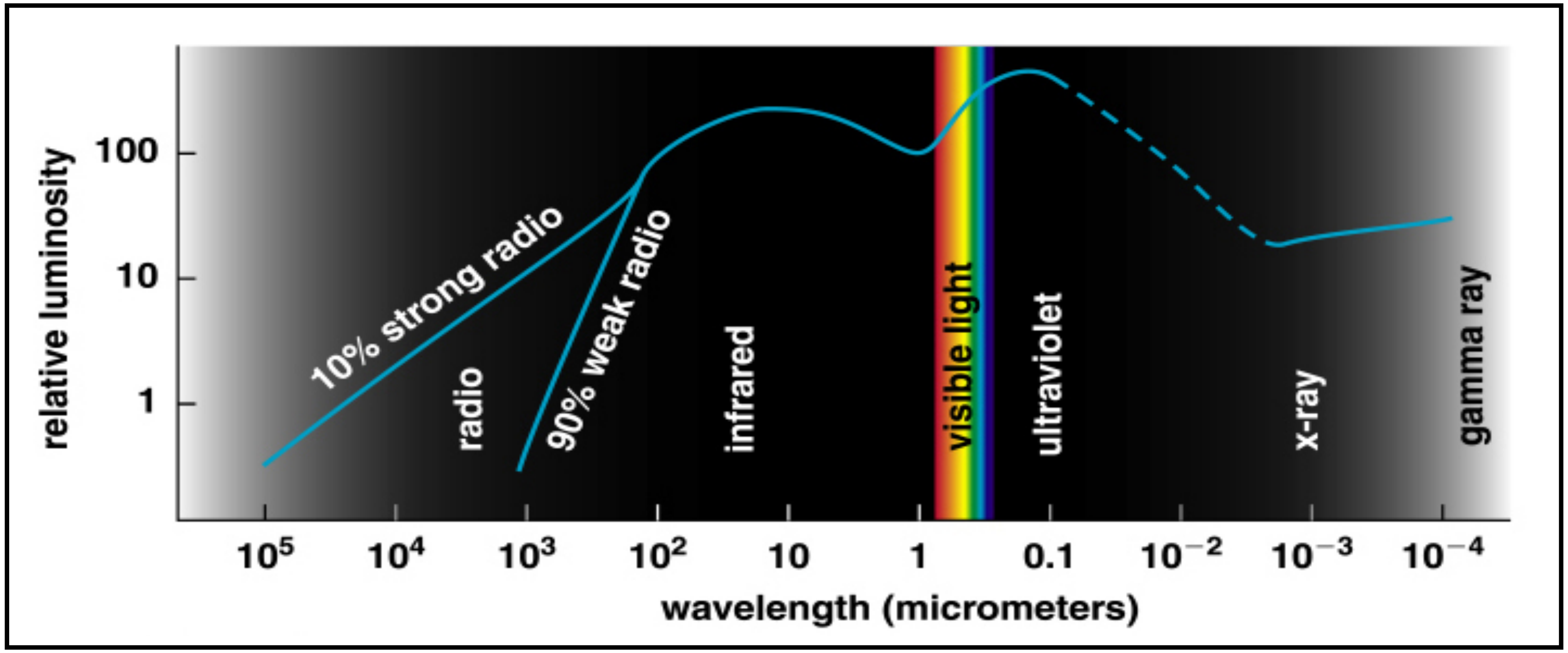

Radio-quiet AGNs

- $L_{radio} \sim 10^3\ L_{radio\ Milky\ Way}$
- the host galaxy is generally a spiral
- Jets/flows at small scale (<kpc)

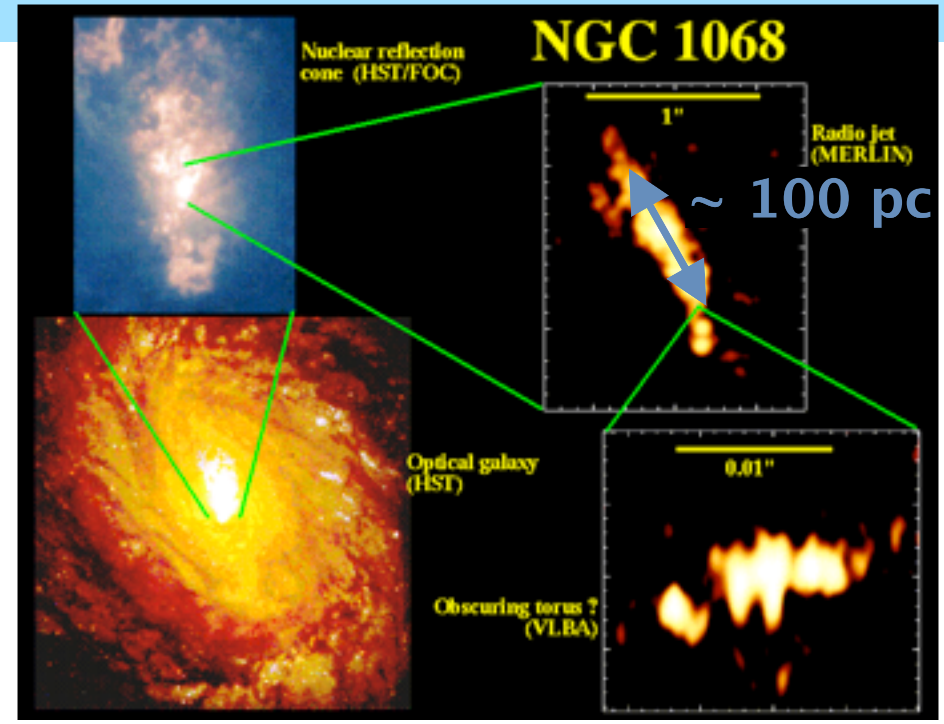

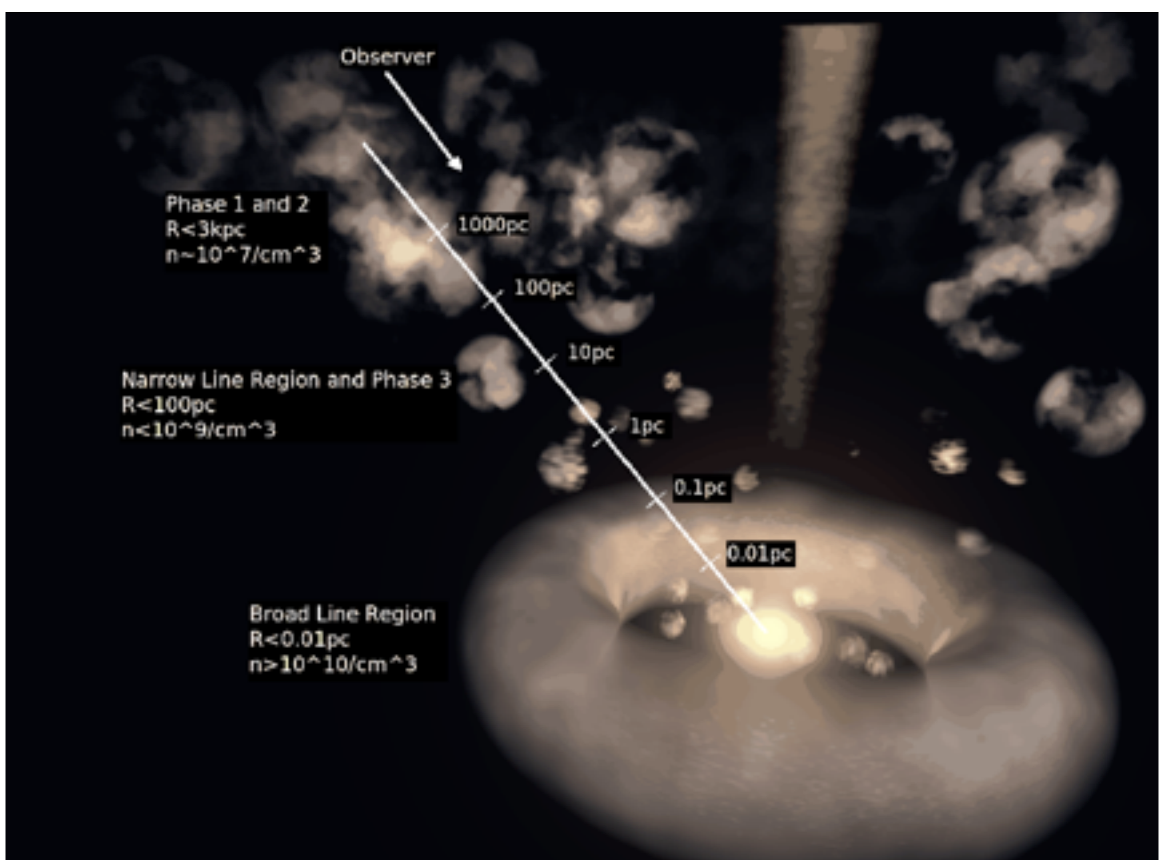

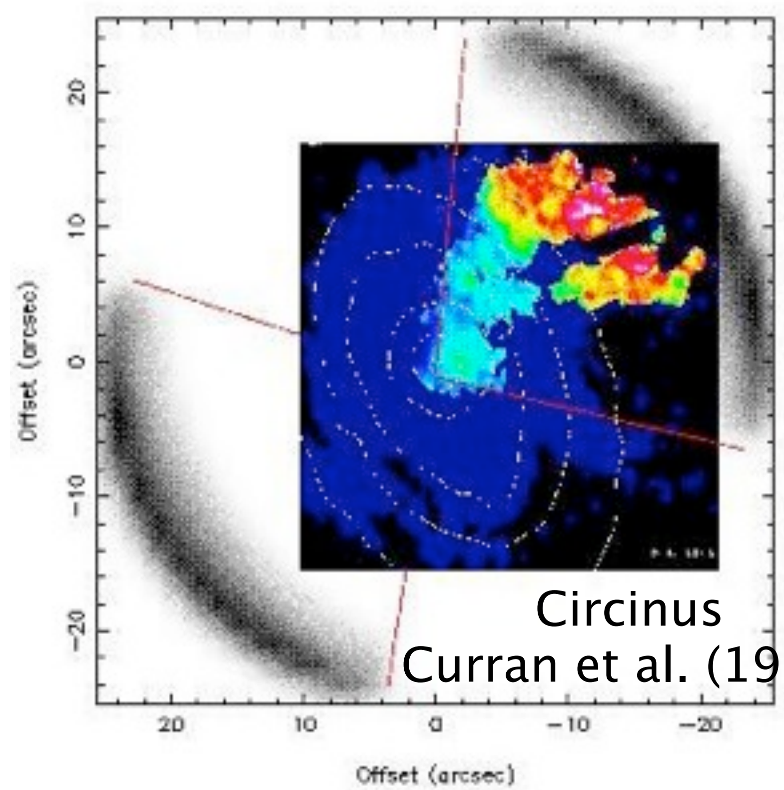

Circinus
Curran et al. (1999)

Why observing in X-rays?

AGNs emit a large part of their energy in X–γ

⇨ $L_{X\text{-}\gamma} \sim L_{bol}$

The fastest variabilities are observed in X–γ

⇨ light minute region size

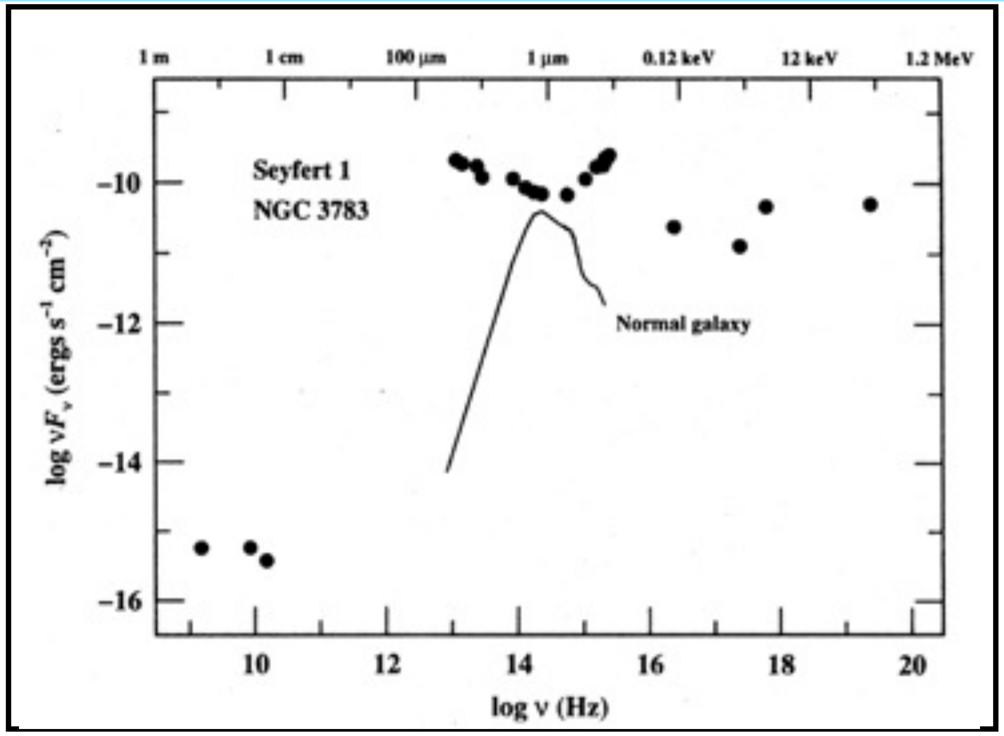

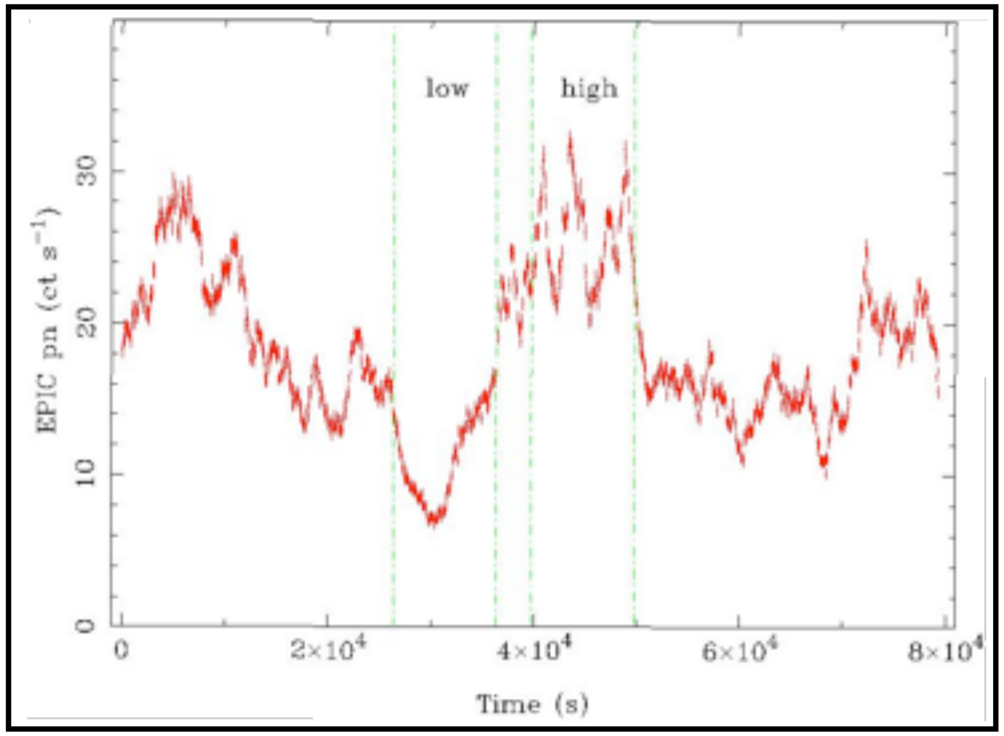

UV-X-ray spectrum

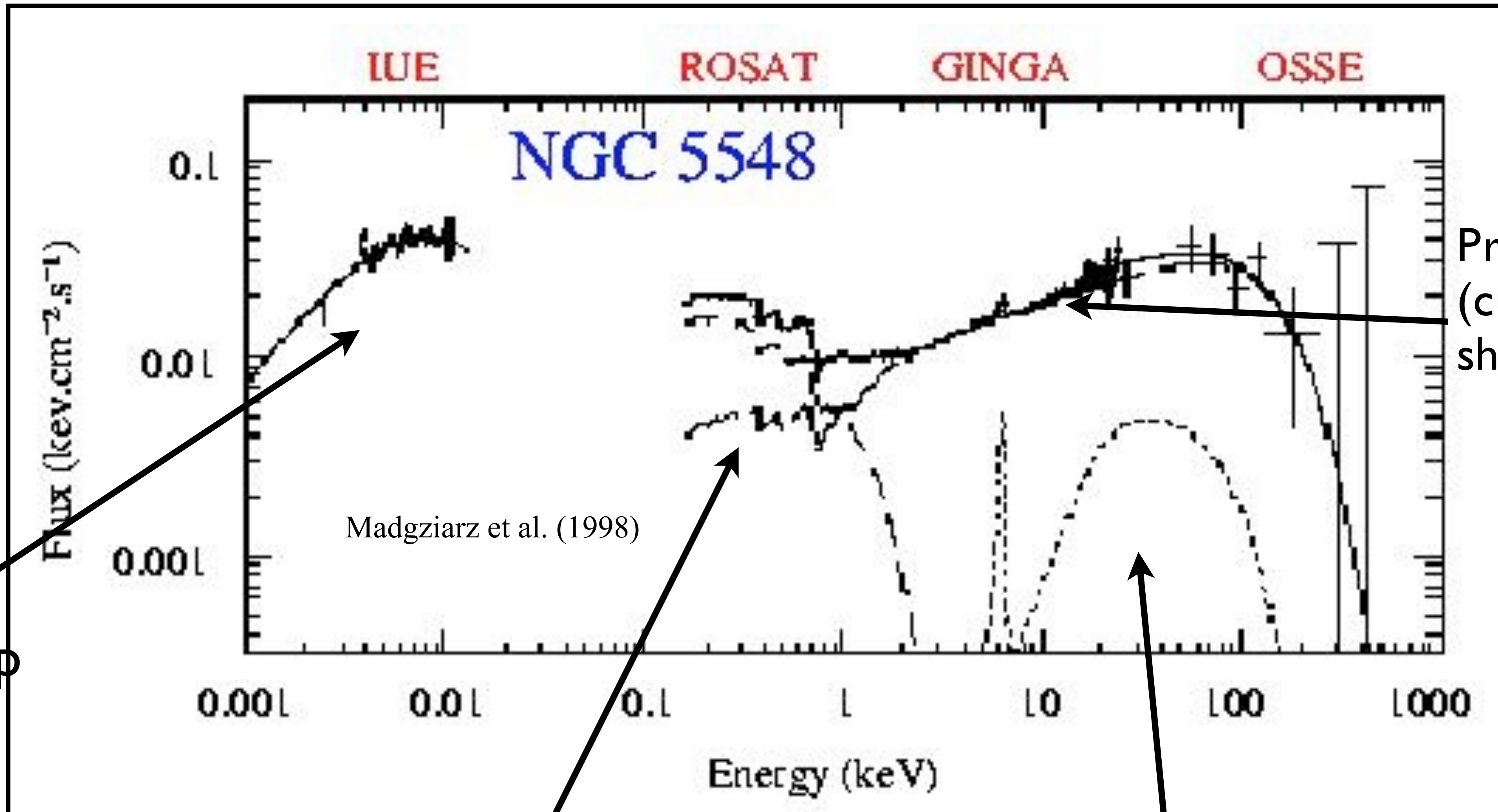

Primary continuum (cut-off power law shape)

Blue bump

soft X-ray excess
and warm absorber

Reflection components:
- iron line
- hump peaking at 30 keV

Beyond the standard accretion disc model

- The accretion disc emission explains the big blue bump but cannot explain the observed X-ray emission

- We need the presence of a hot gaz radiating in X-ray:
  ➡ the corona

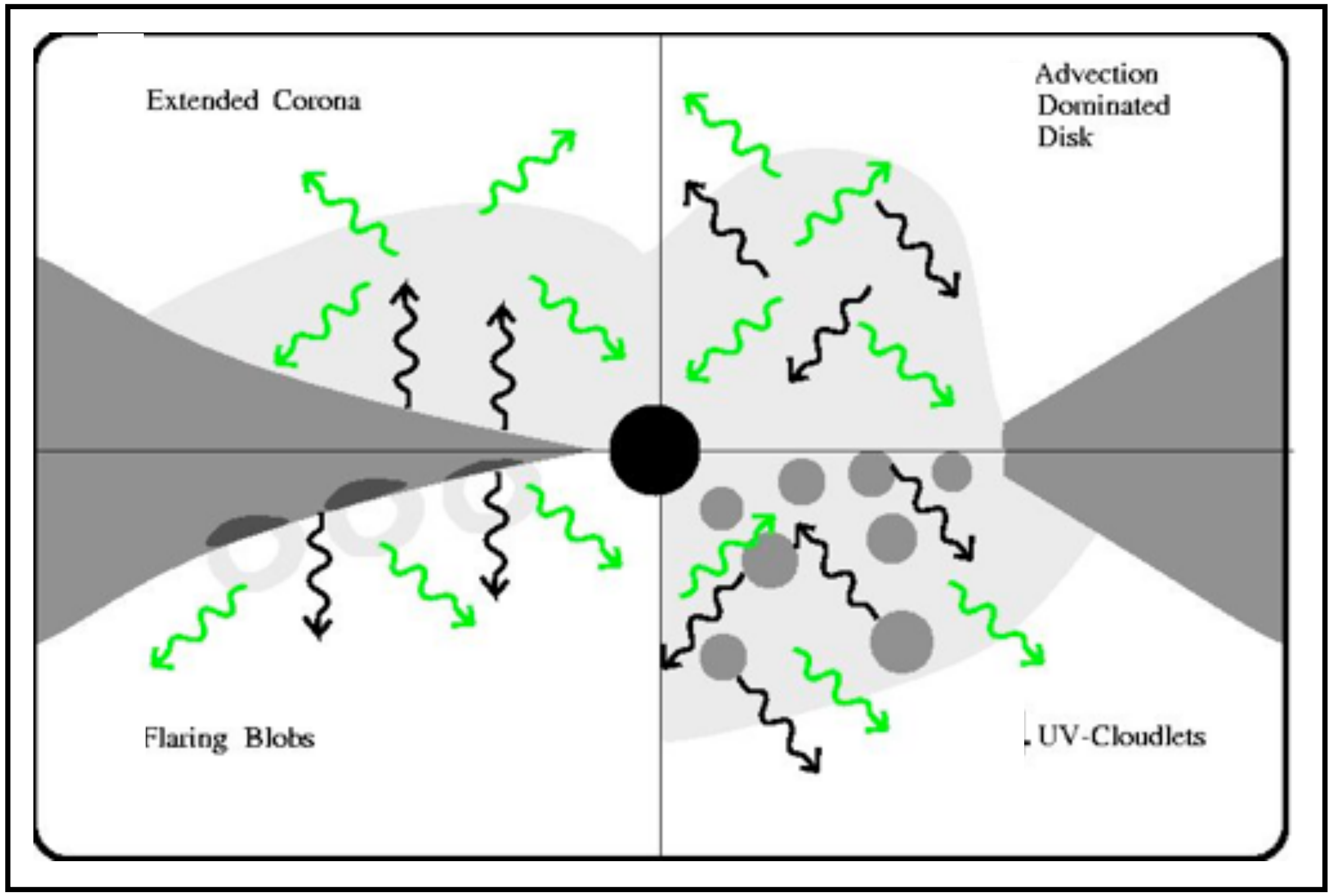

UV-X-ray emission origin

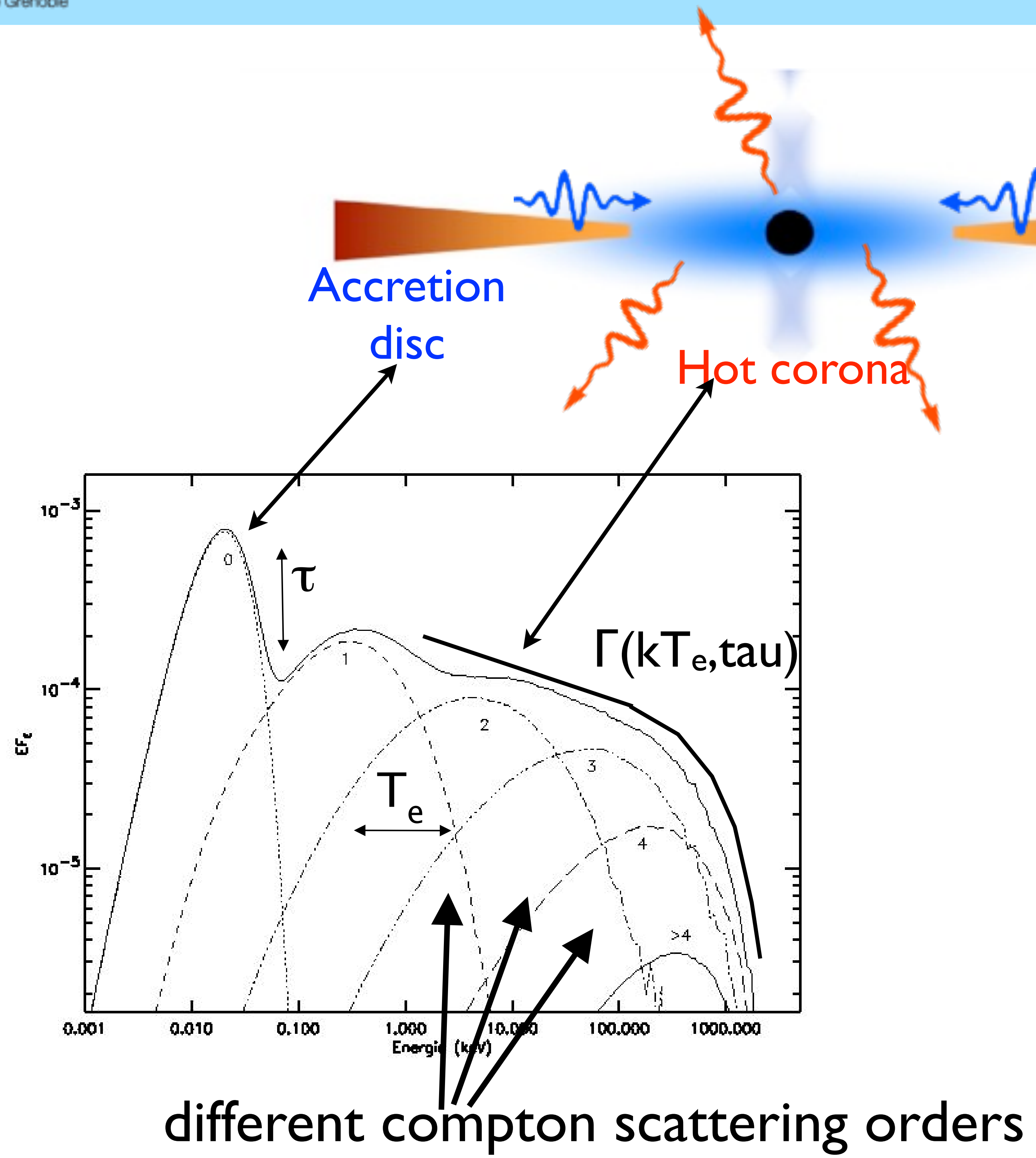

Thermal inverse Compton

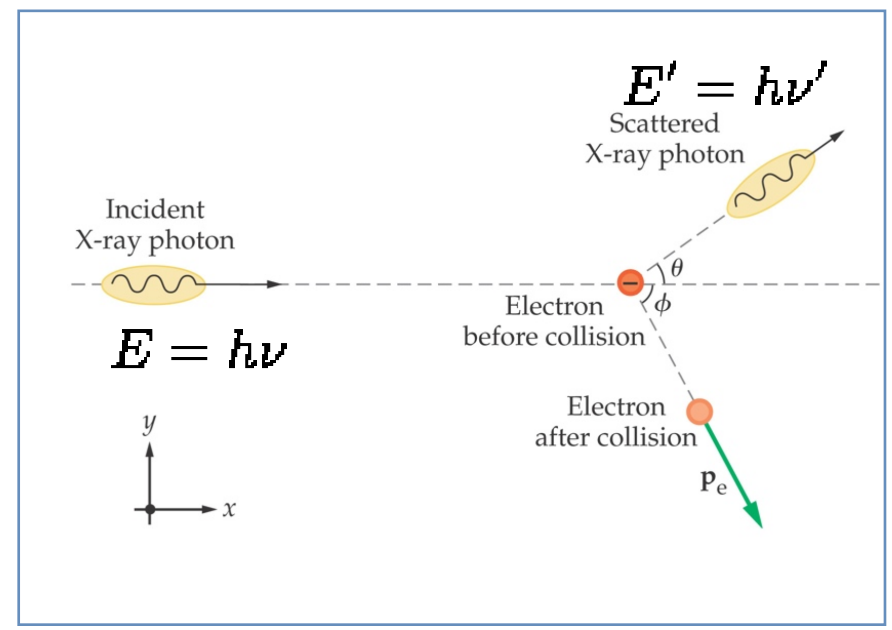

Energetics dependency

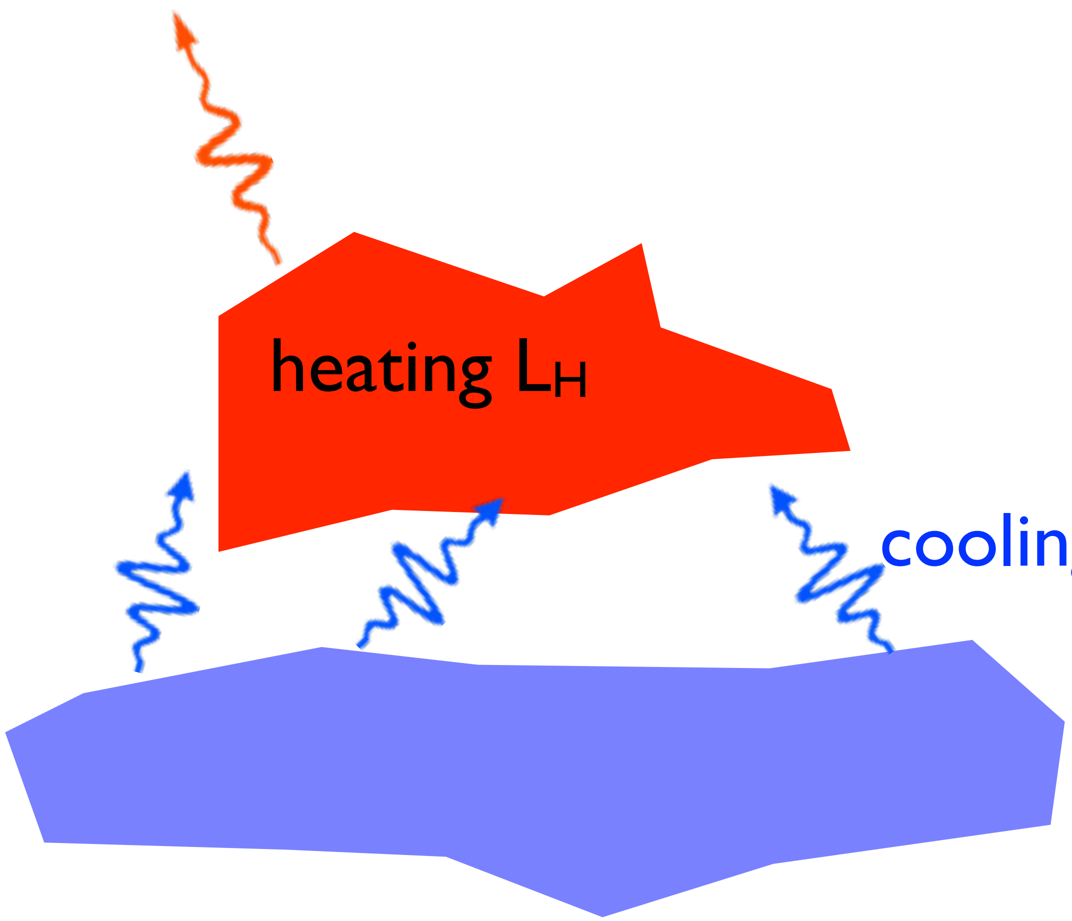

⇔

Spherical geometry, τ=0.1 but different Heating/Cooling ratios

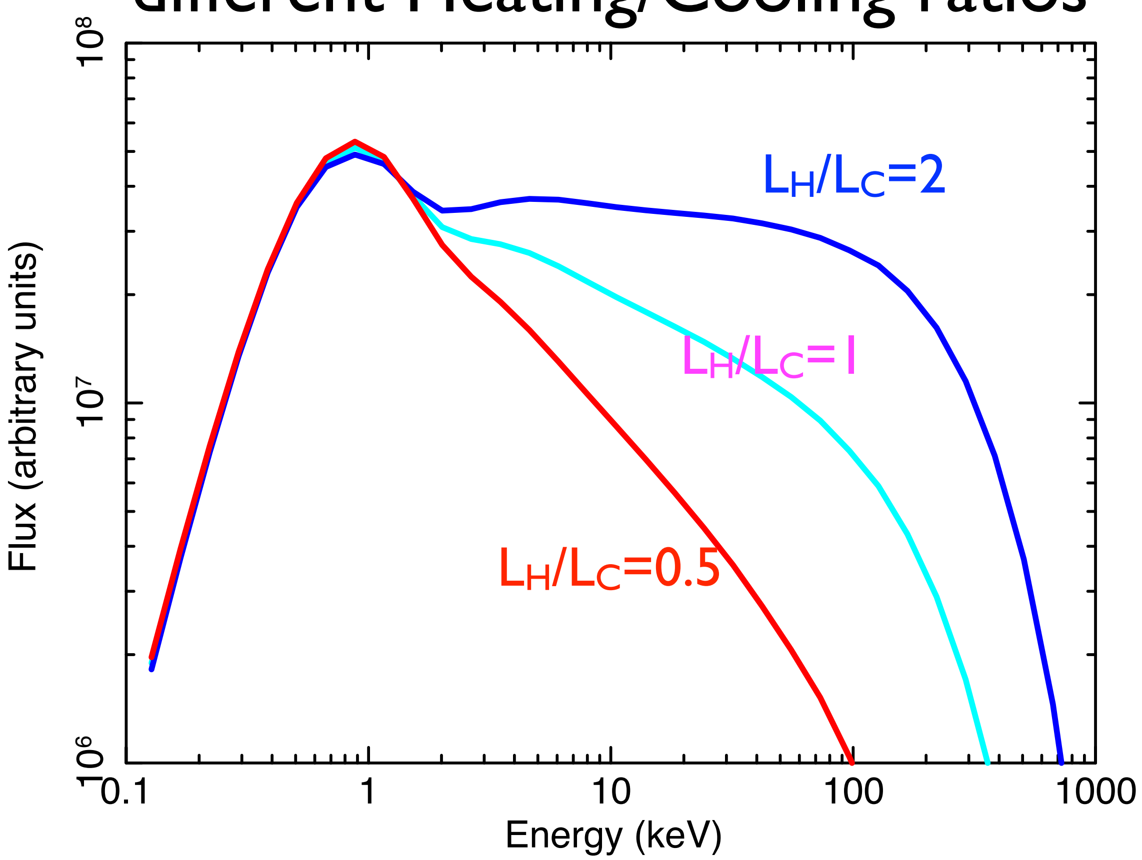

Slab corona above a passive disc ➡ $L_H/L_C=1$

Radiative equilibrium

If the 2 phases are in radiative equilibrium, the corona temperature and optical depth follow a univocal relationship.

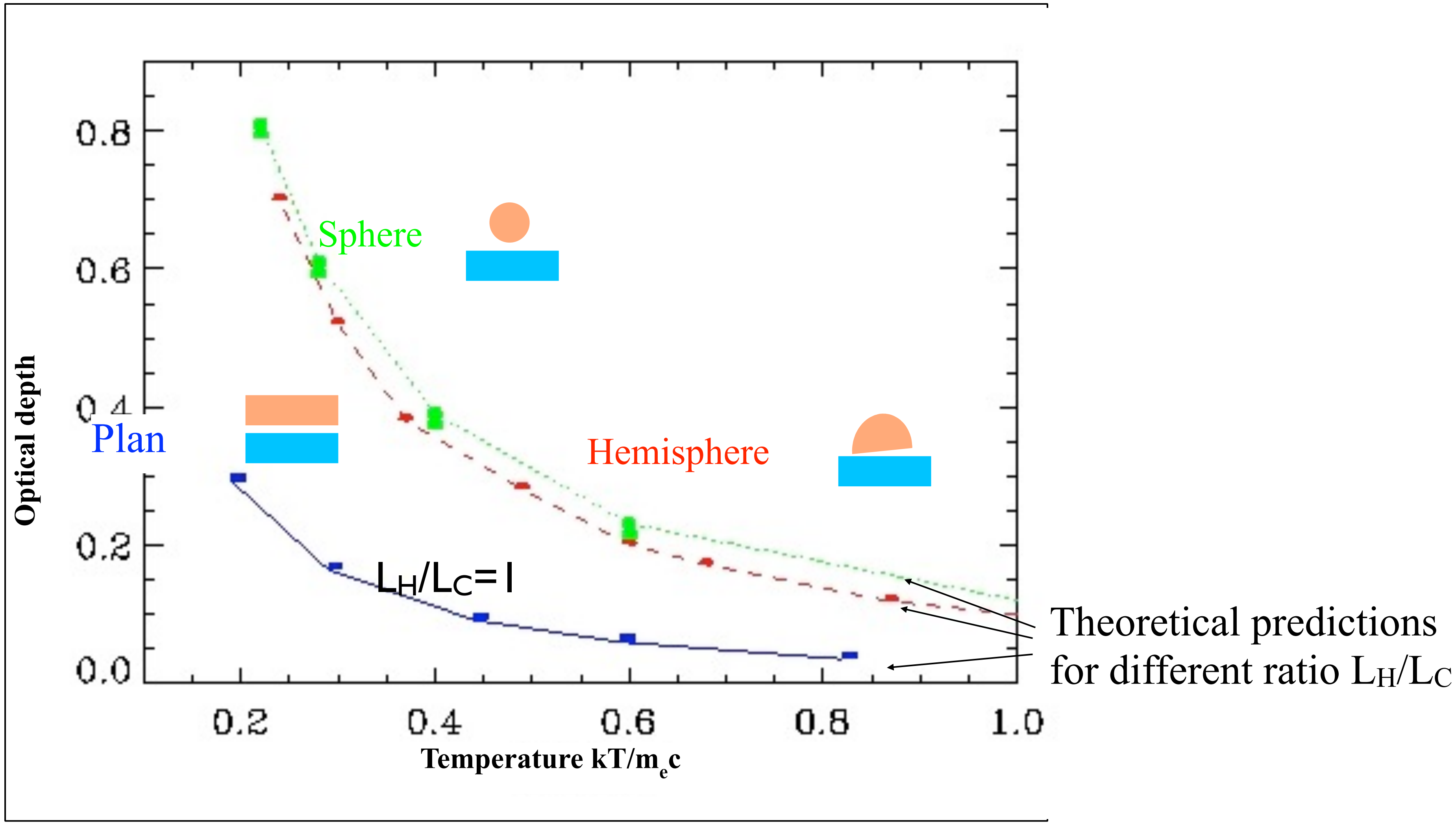

Radiative equilibrium

If the 2 phases are in radiative equilibrium, the corona temperature and optical depth follow a univocal relationship.

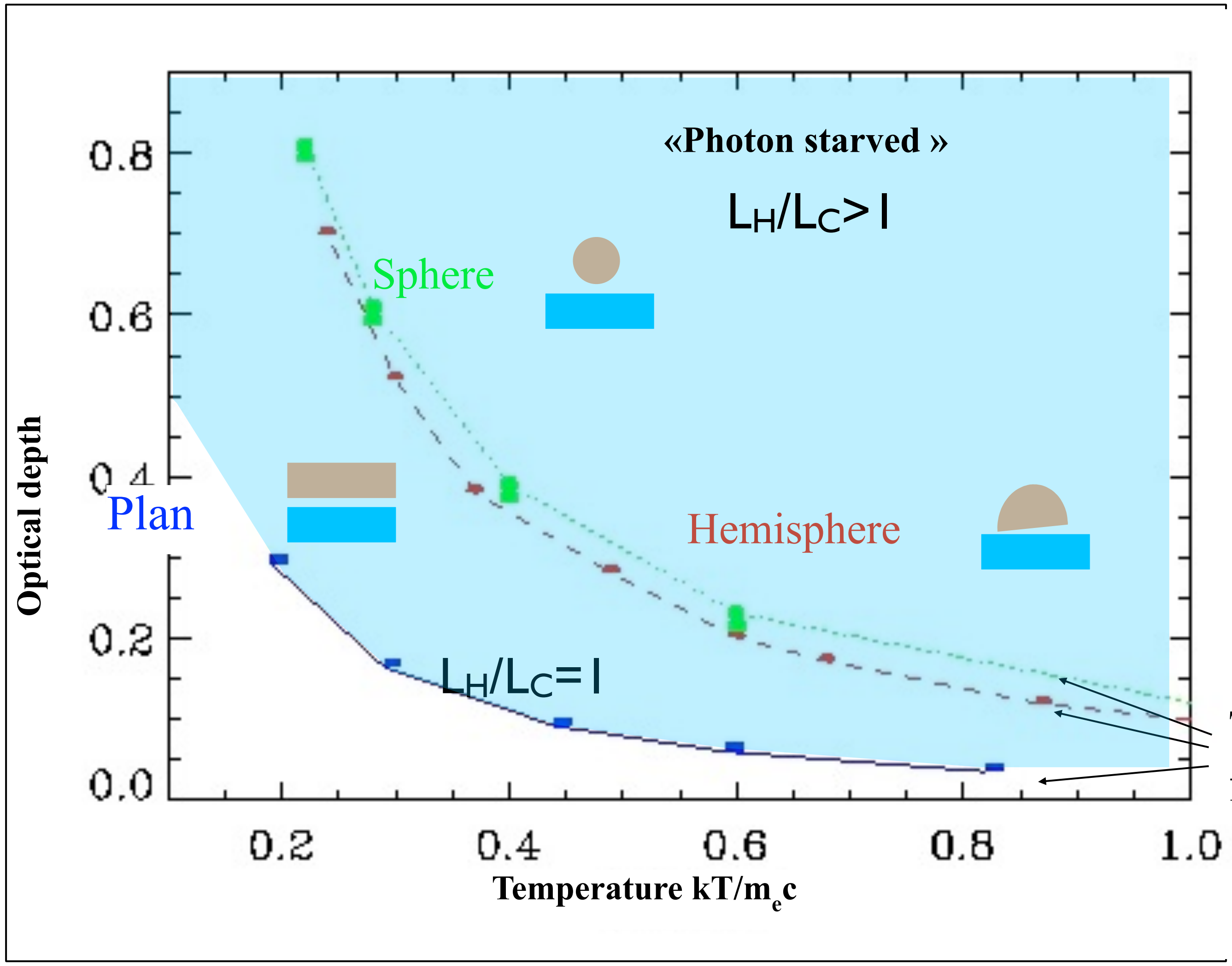

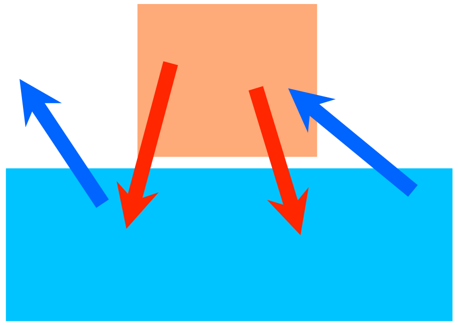

Radiative equilibrium

If the 2 phases are in radiative equilibrium, the corona temperature and optical depth follow a univocal relationship.

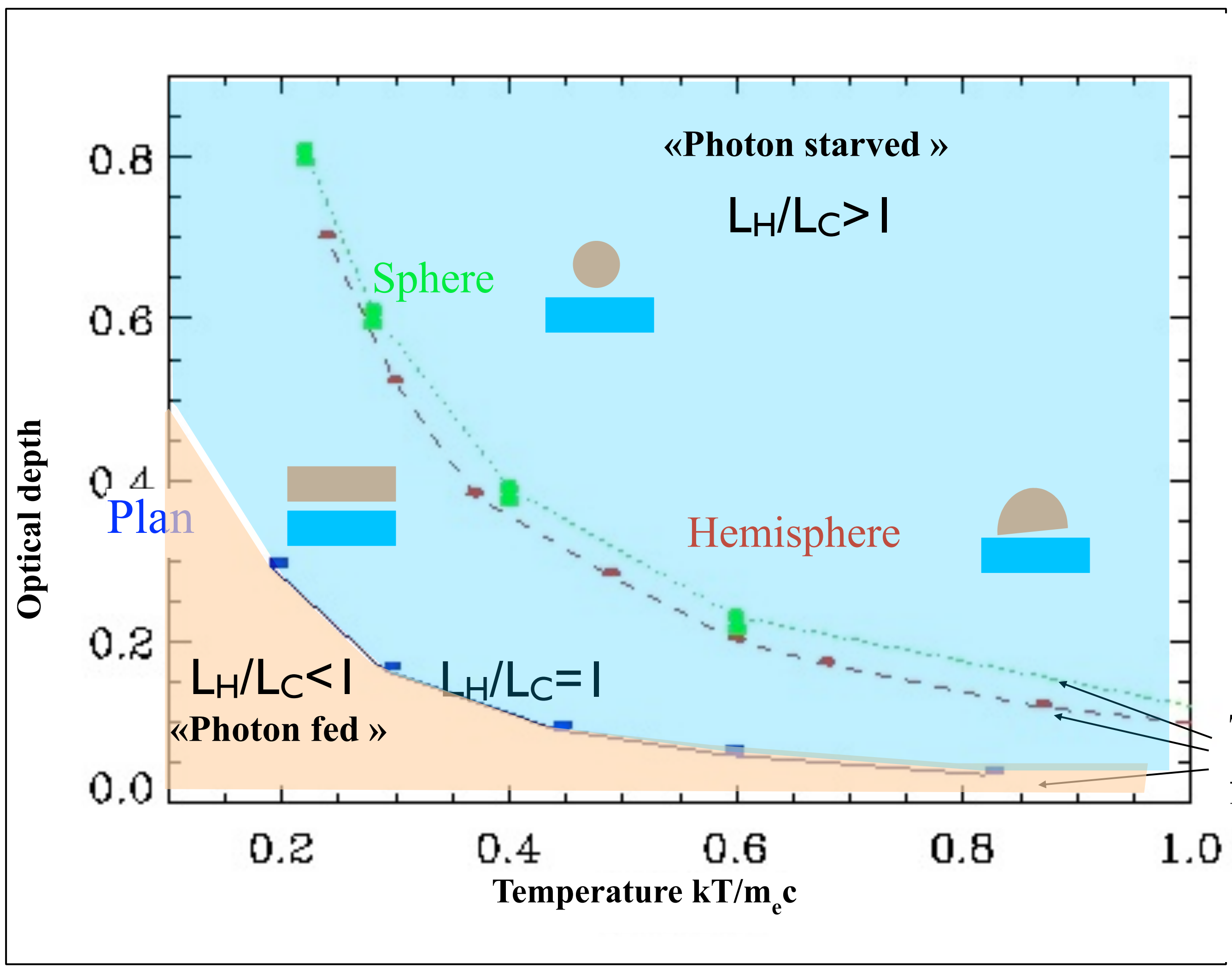

Theoretical predictions for different ratio L_H/L_C

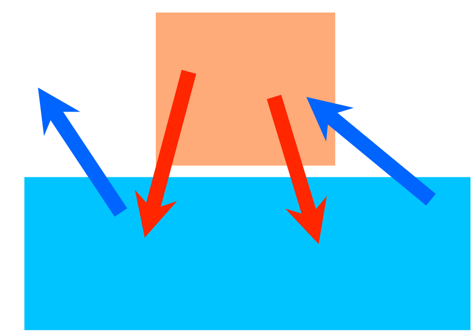

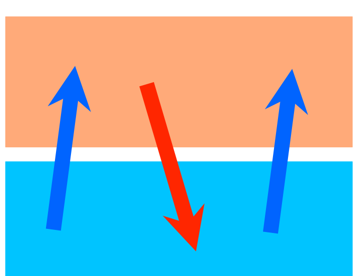

Ex: intrinsic disc emission

Reflection Components

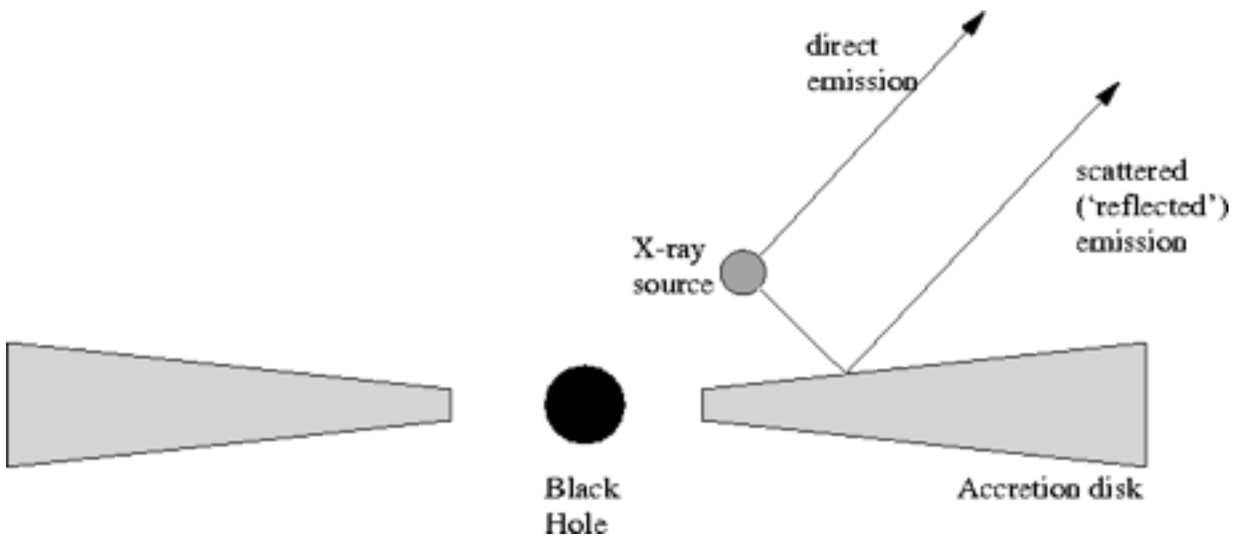

Simulation

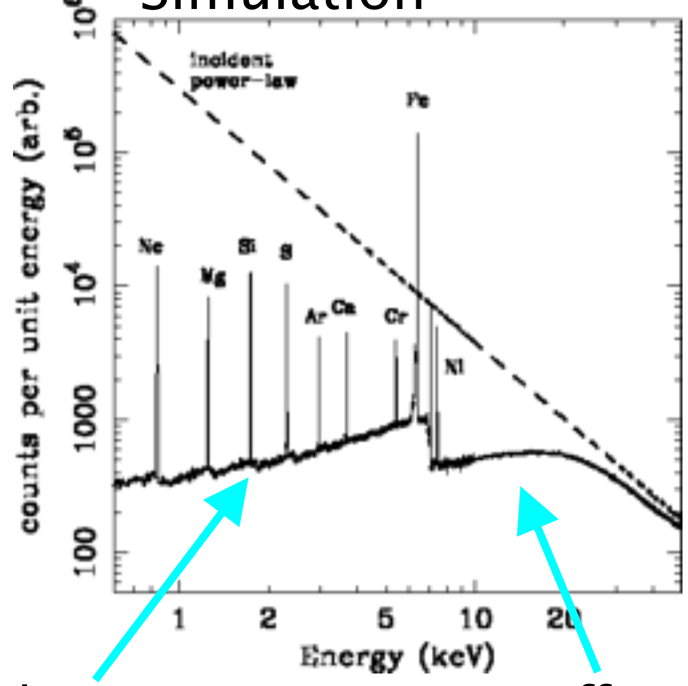

Absorption
Photoélectriques

Effets
Klein–Nishina

Observation

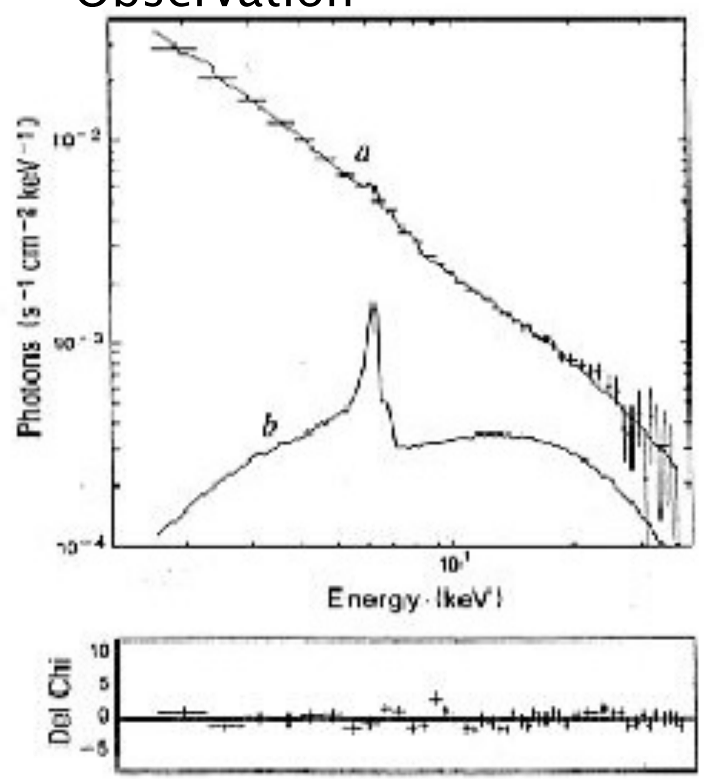

Pounds et al. (1990)

Iron line broadening

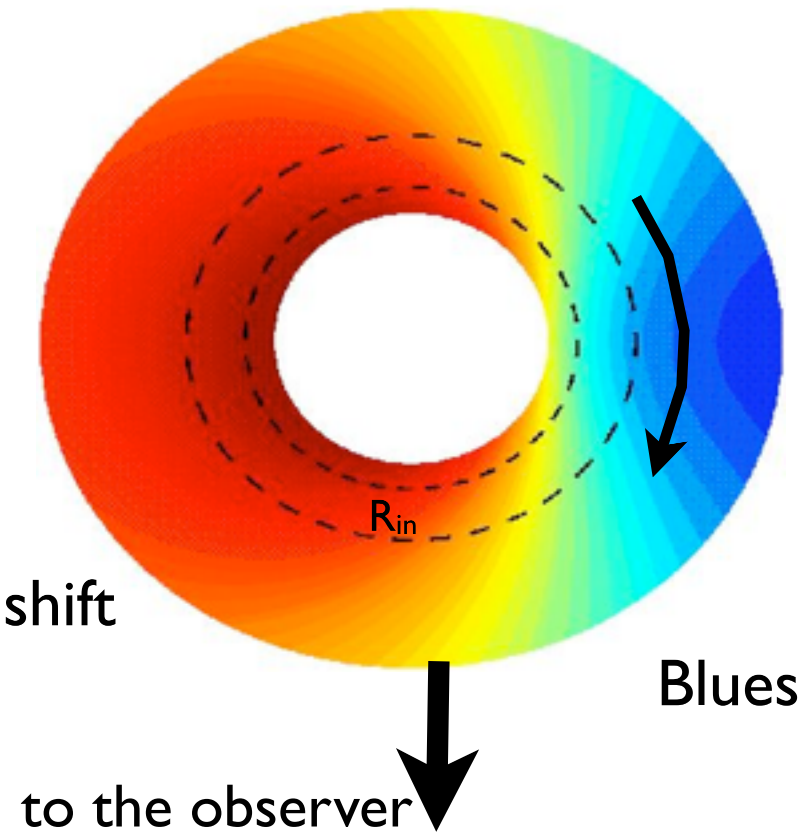

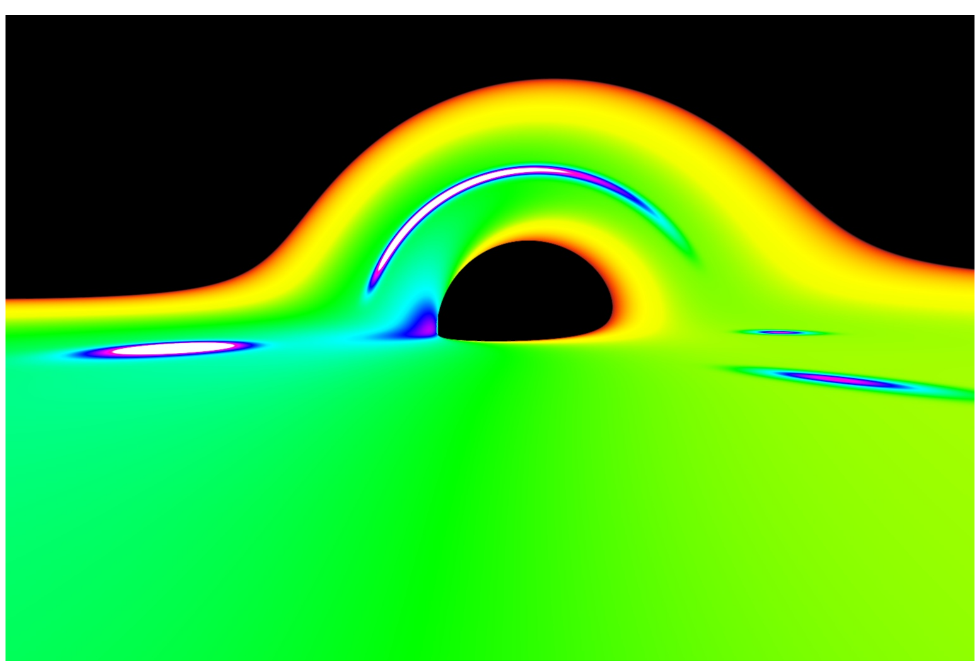

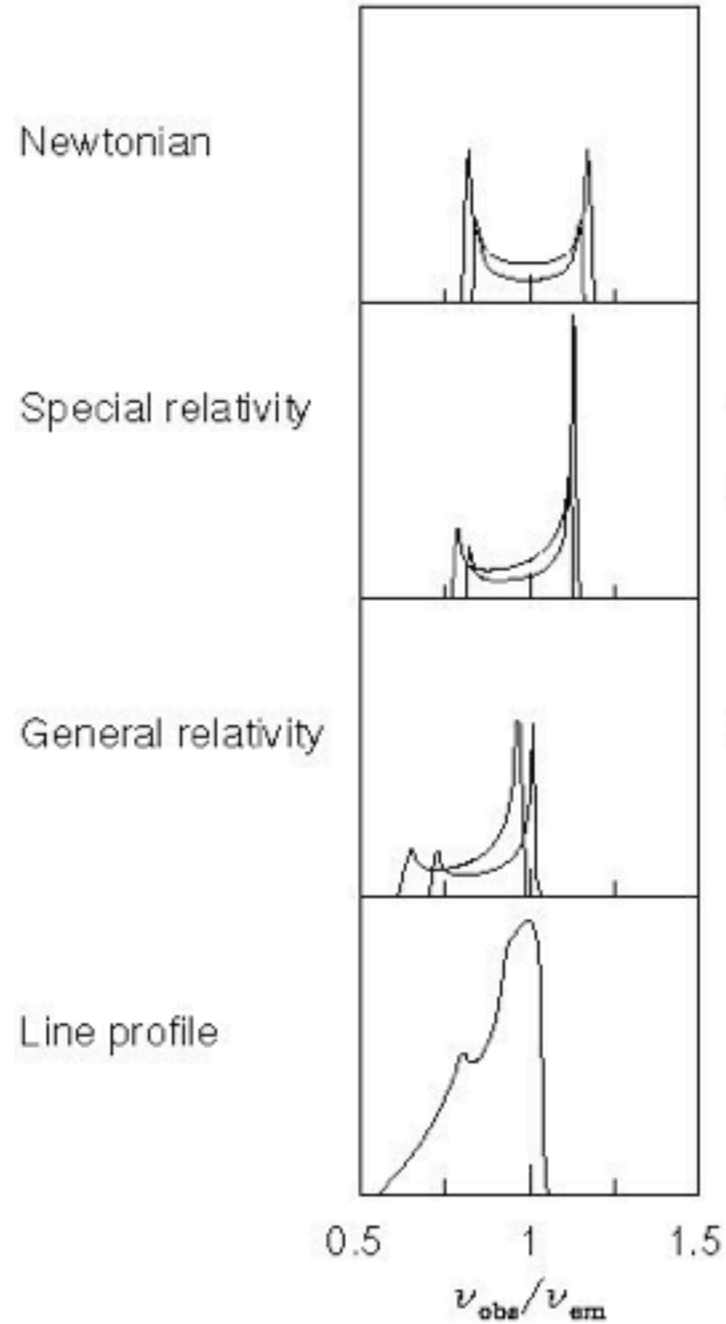

Fabian et al. (1989)

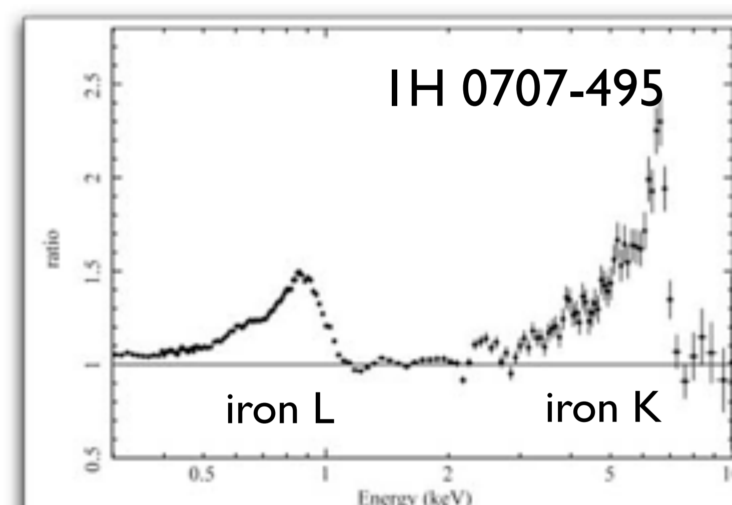

Fabian et al. (2009)

Soft X-ray Excess

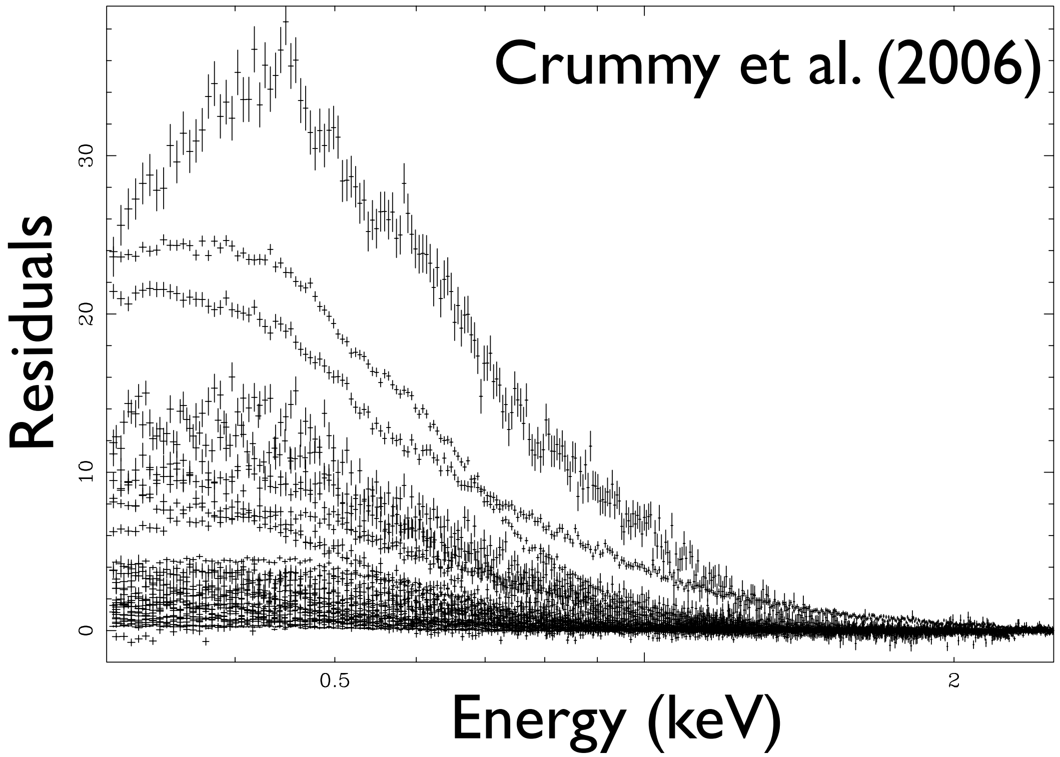

Origin still debated....

- Blurred ionised reflection

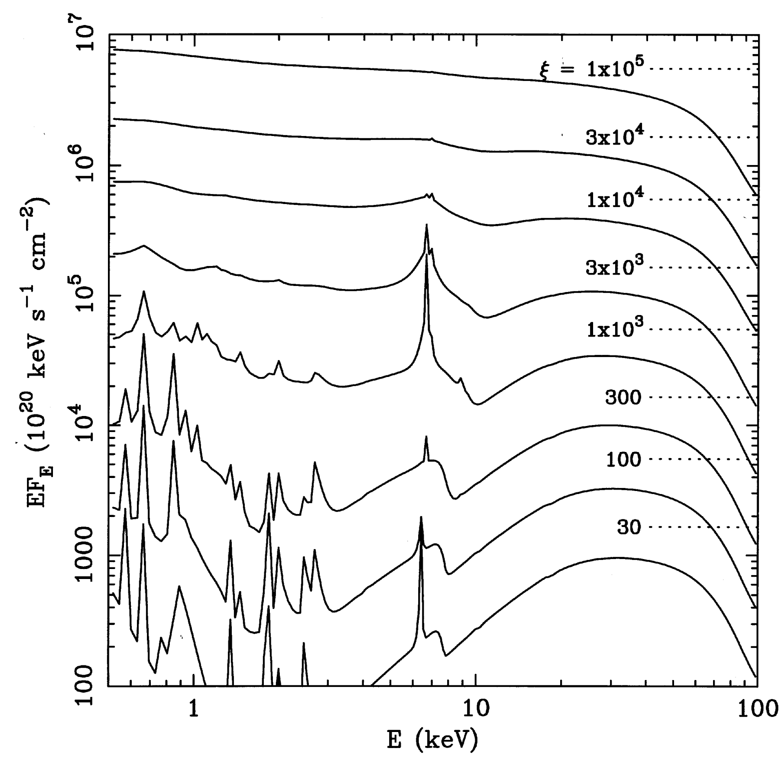

- Disc thermal comptonisation in a warm (T~ 1 keV) optically thick (τ~10) corona

Warm Absorber: outflows

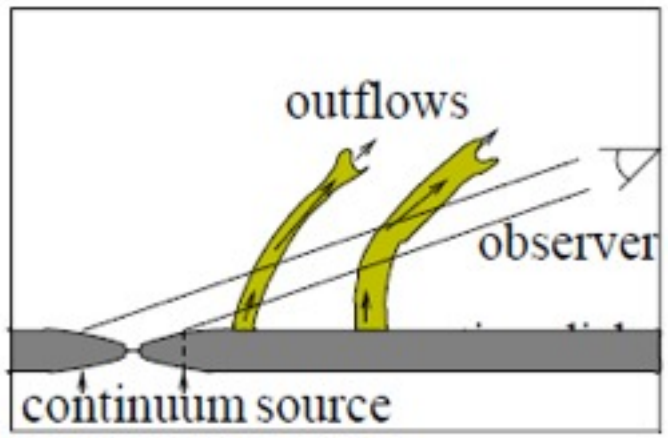

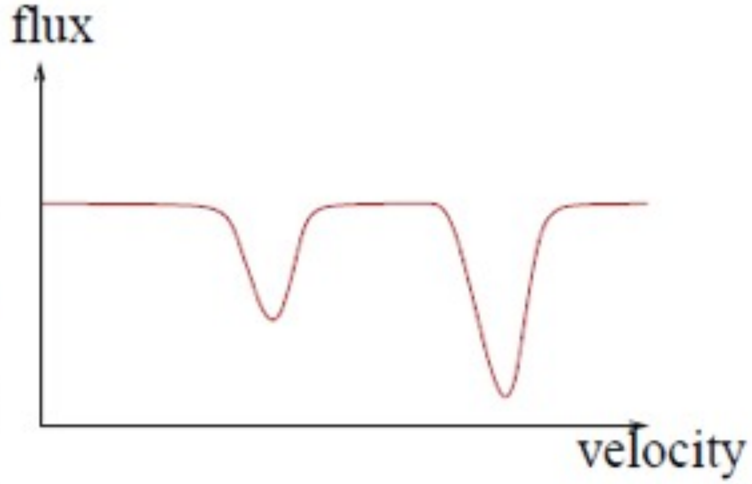

- Photo-ionised gas
- v = -100 to -1000 km/s
- Seen through line and continuum absorption

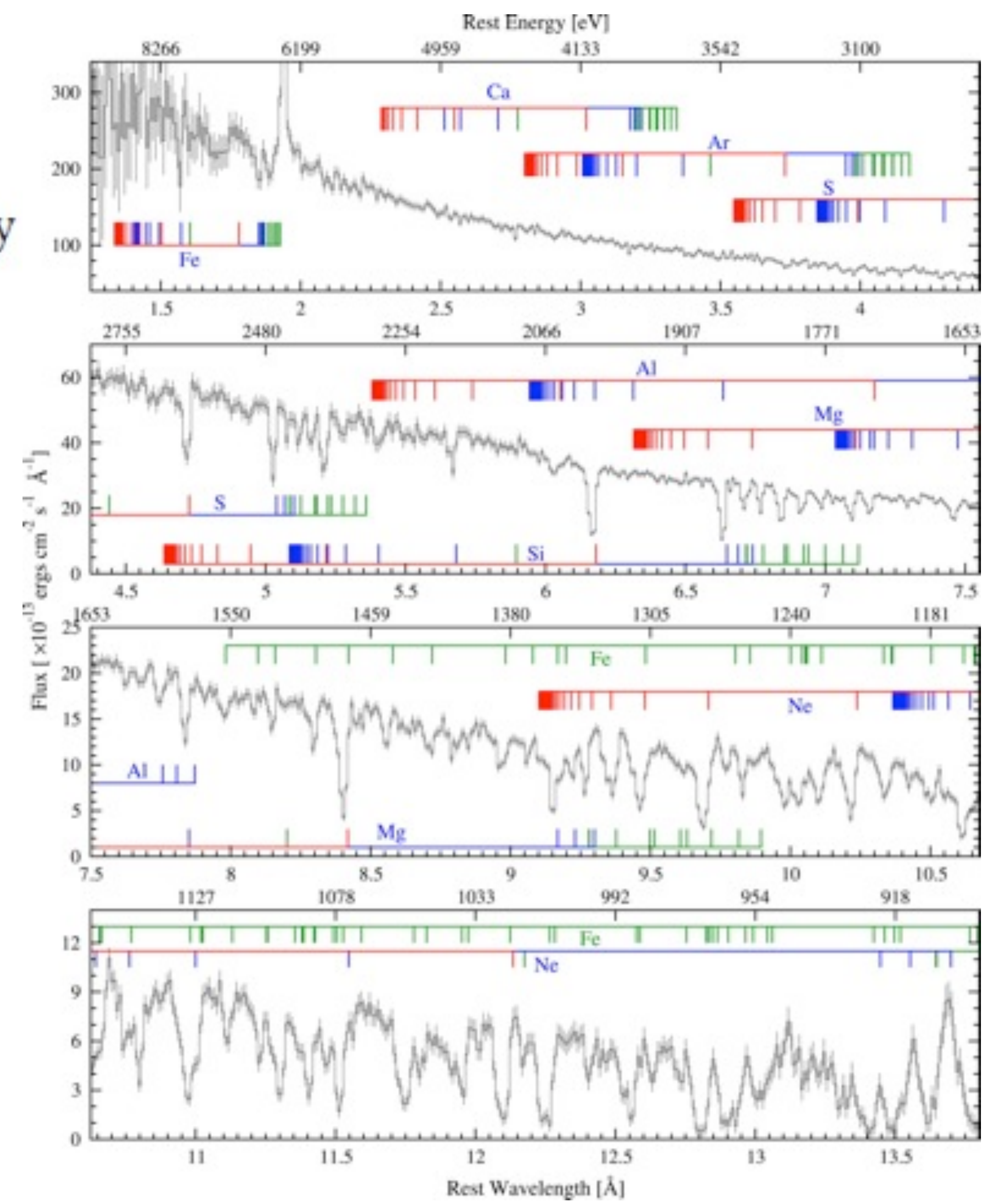

(NGC 3783, Kaspi et al. 2003)

Outflows composition: method

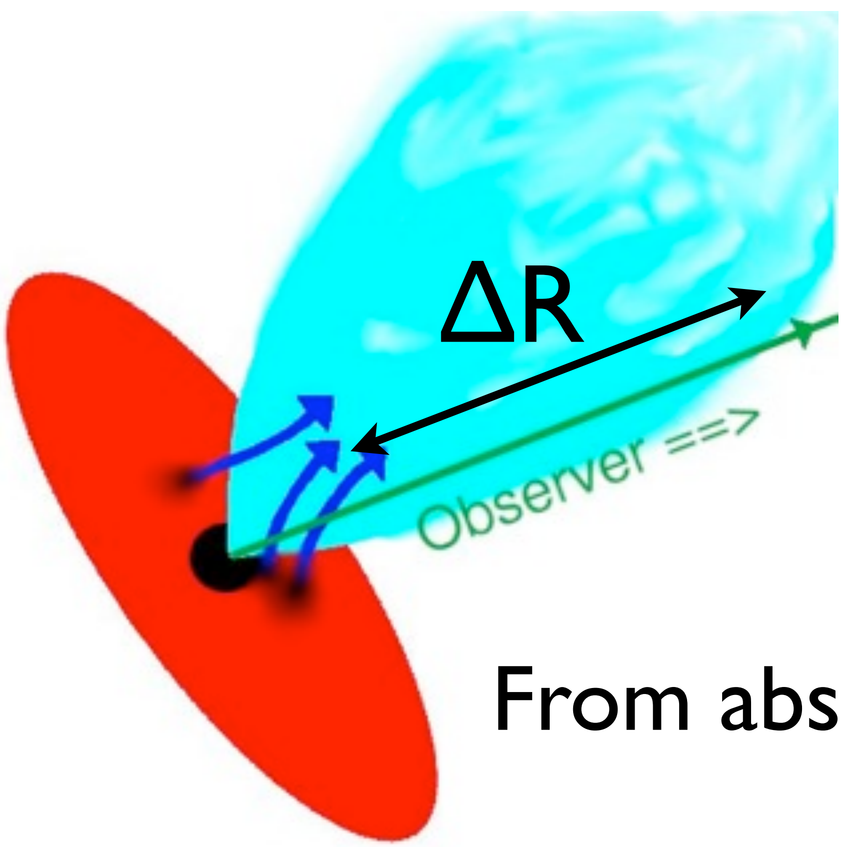

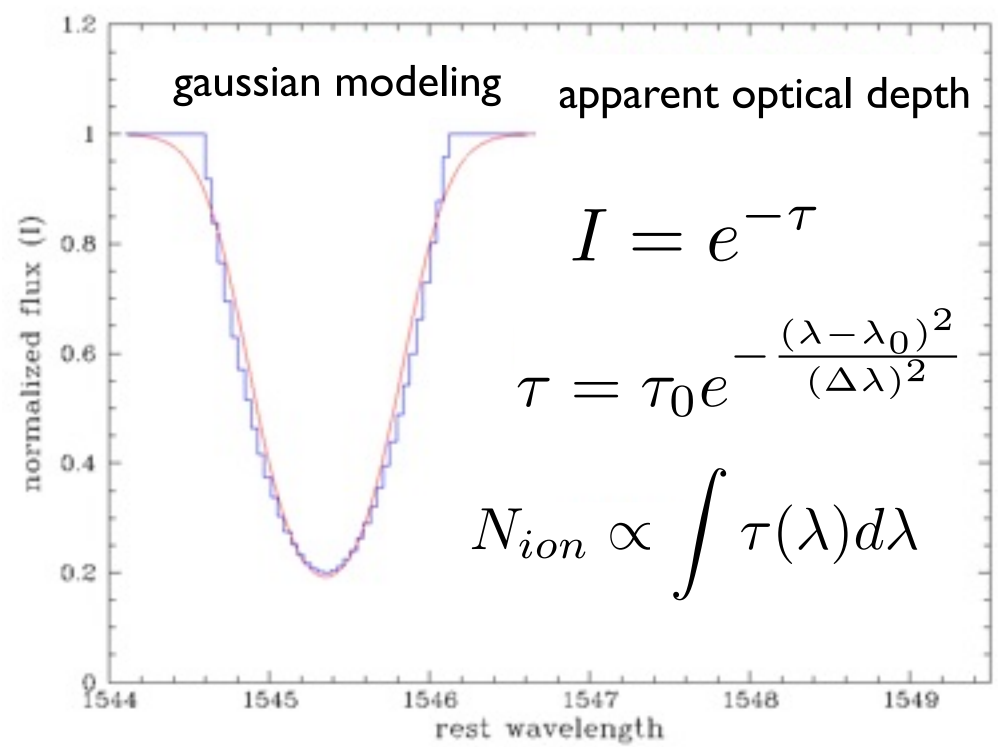

From absorption lines measurement ➡ N_{ion}^{Obs}

ion column density on the line of sight

$$N_{ion}^{Th} = \left(\frac{N_{ion}^{Th}}{N_Z}\right)\left(\frac{N_Z}{N_H}\right) N_H \qquad \text{with} \qquad N_H = n_H \Delta R$$

abundance

fundamental state

hydrogen column density

Outflows composition: method

- The ionization states are characterized by the ionisation parameter $\xi = \dfrac{L}{n_H r^2}$

Photoionisation code $\rightarrow$ $\boxed{\dfrac{N_{ion}^{Th}}{N_Z} = f(\xi)}$

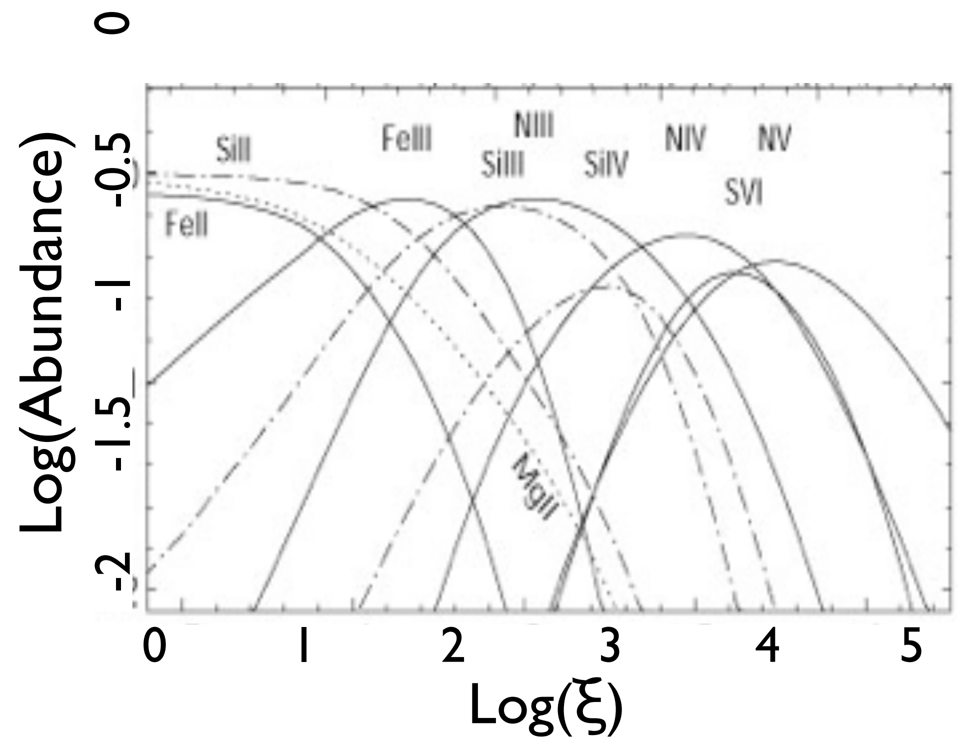

Outflows composition: method

- The ionization states are characterized by the ionisation parameter $\xi = \frac{L}{n_H r^2}$

Photoionisation code $\rightarrow$ $\boxed{\frac{N_{ion}^{Th}}{N_Z} = f(\xi)}$

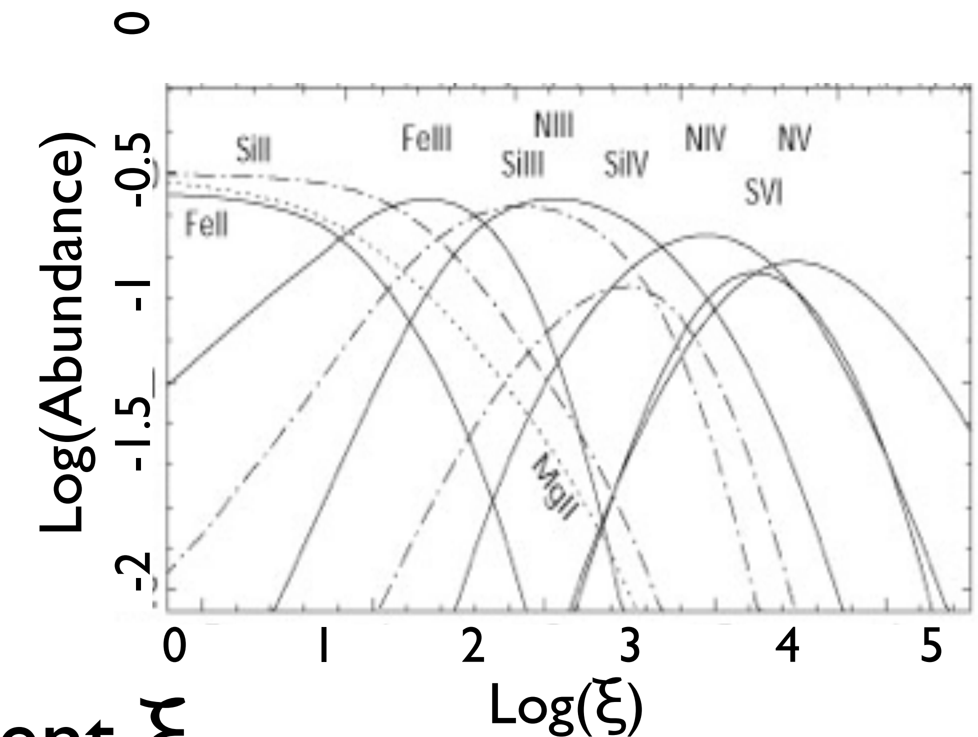

- But we can have different media with different ξ

$\boxed{\text{Absorption Measure Distribution } N_H(\xi)}$

Outflows composition: method

- The ionization states are characterized by the ionisation parameter $\xi = \frac{L}{n_H r^2}$

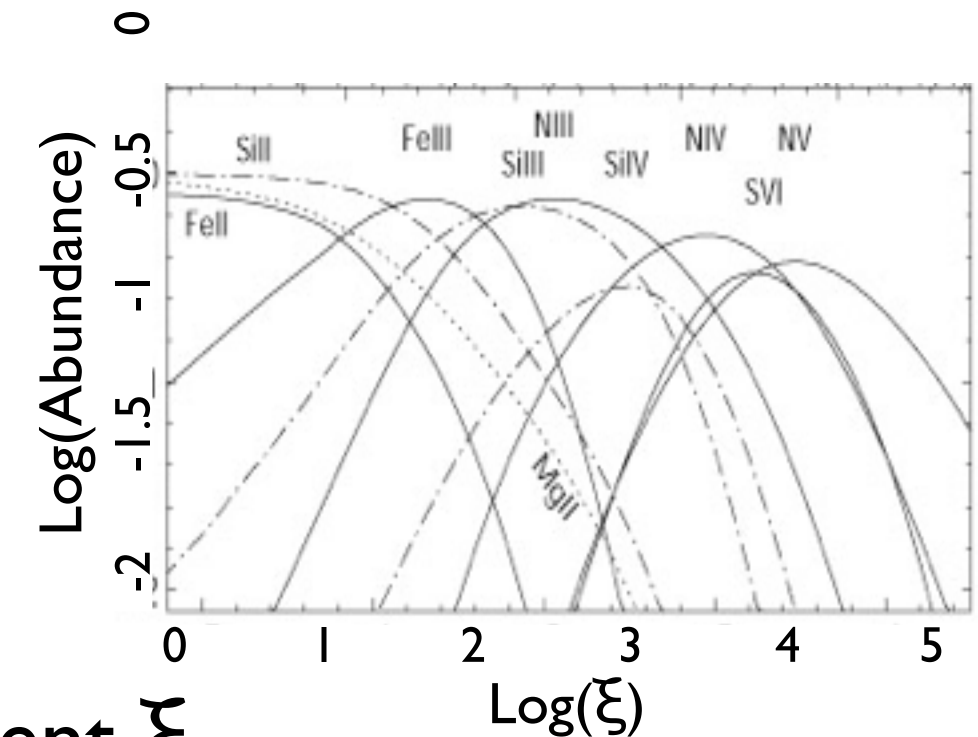

Photoionisation code $\rightarrow$ $\boxed{\frac{N_{ion}^{Th}}{N_Z} = f(\xi)}$

- But we can have different media with different ξ

$\boxed{\text{Absorption Measure Distribution } N_H(\xi)}$

$$\rightarrow \quad N_{ion}^{Th} = \int_0^\infty f(\xi) \left(\frac{N_Z}{N_H}\right) \frac{dN_H}{d\xi} d\xi$$

$$\boxed{N_{ion}^{Th} = N_{ion}^{Obs} \quad \rightarrow \quad N_H(\xi) \text{ and } \left(\frac{N_Z}{N_H}\right)}$$

Thermal Equilibrium

When the condition of thermal equlibrium is imposed, then the temperature is determined as a function of the ionization parameter.

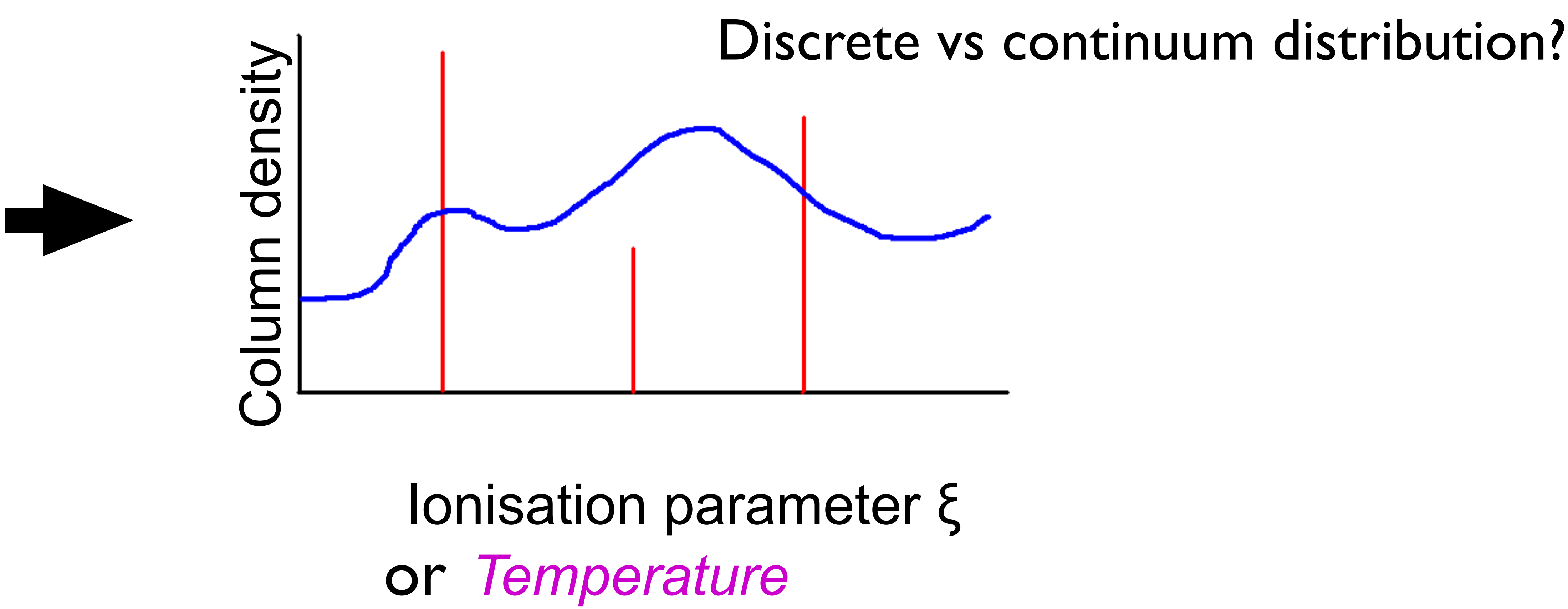

"Reverberation" mapping

- Photo-ionization modeling ➔ $\xi = L/nr^2$
- L obtained from spectrum

  ➔ only the product nr^2 known, not r or n

“Reverberation” mapping

- Photo-ionization modeling ➔ $\xi = L/nr^2$
- L obtained from spectrum

  ➔ only the product nr^2 known, not r or n

Different methods may help defining r or n. Here we focus on “reverberation” mapping:

- If L increases for gas at fixed n and r, then $\xi = L/nr^2$ increases

  ➔ change in ionisation balance

  ➔ column density changes

  ➔ transmission changes
- Gas has finite ionisation/recombination time t_r (varies like $\sim 1/n$)

  ➔ measuring delayed response yields t_r ➔ n ➔ r

The case of Mrk 509

- Seyfert 1, $M_{BH} \sim 10^8 M_{sun}$
- One of the brigtest Seyfert in X-rays
- X-ray spectrum with all the common spectral components
  - ✓ Big blue bump
  - ✓ iron line (+ reflection hump)
  - ✓ soft X-ray excess
  - ✓ WA

HST image of Mrk 509

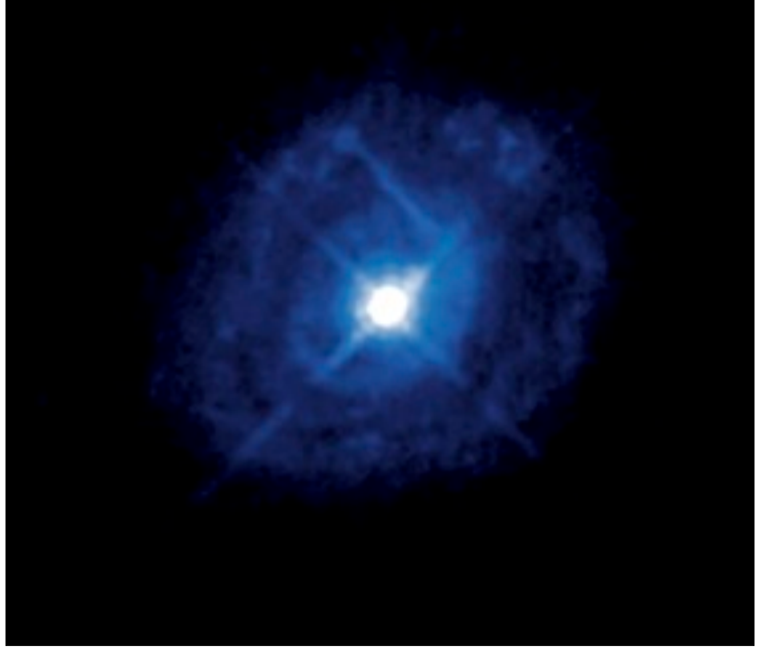

The case of Mrk 509

- Seyfert 1, $M_{BH} \sim 10^8 M_{sun}$
- One of the brigtest Seyfert in X-rays
- X-ray spectrum with all the common spectral components
  - ✓ Big blue bump
  - ✓ iron line (+ reflection hump)
  - ✓ soft X-ray excess
  - ✓ WA

- Broad band monitoring coordinated by J. Kaastra (SRON, Netherland)

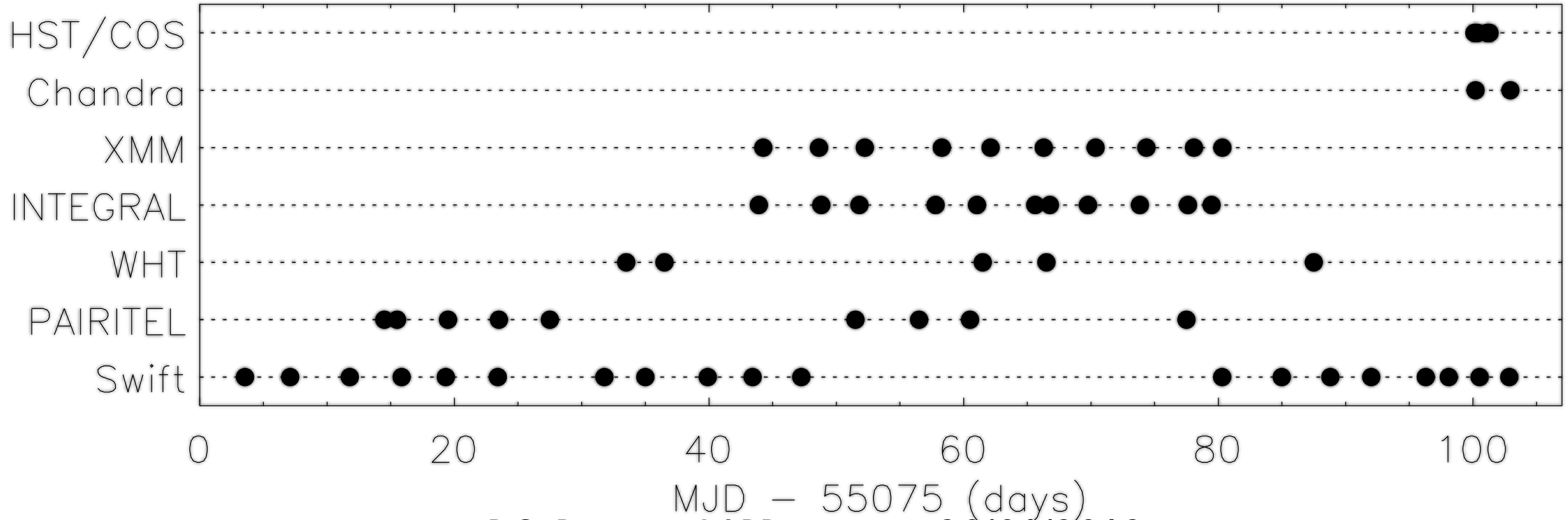

Broad band continuum analysis

Broad band monitoring

- One month XMM/INTEGRAL monitoring (1 obs. every 4 days)

EPIC:0.15 to 15 keV
RGS: spectro. 0.5-2 keV
OM: 2-6 eV

IBIS: 20 keV à 10 MeV
SPI: 20 keV à 8 MeV.
JEMX: 2-20 keV
OMC: optique

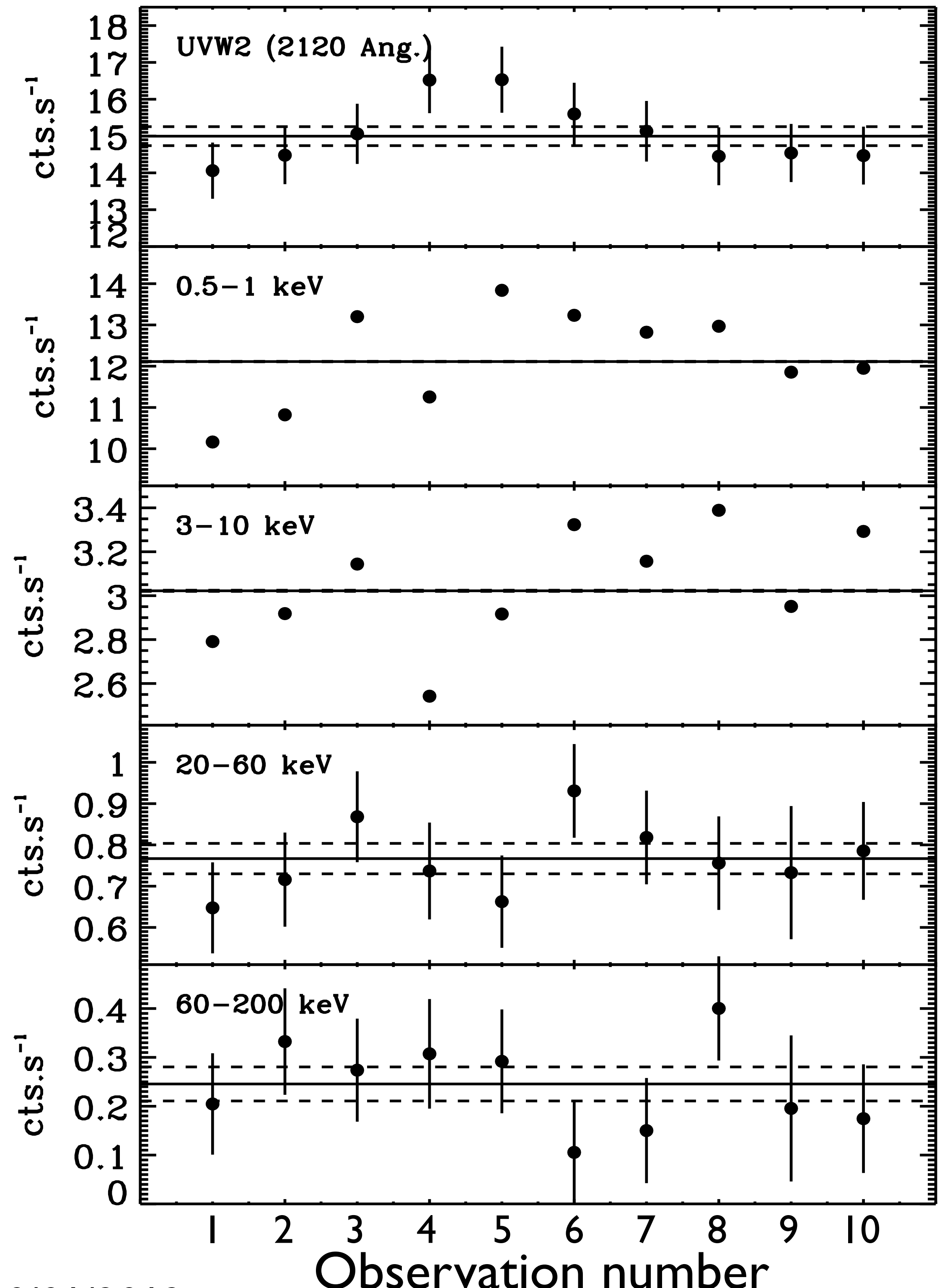

Two independent spectral components?

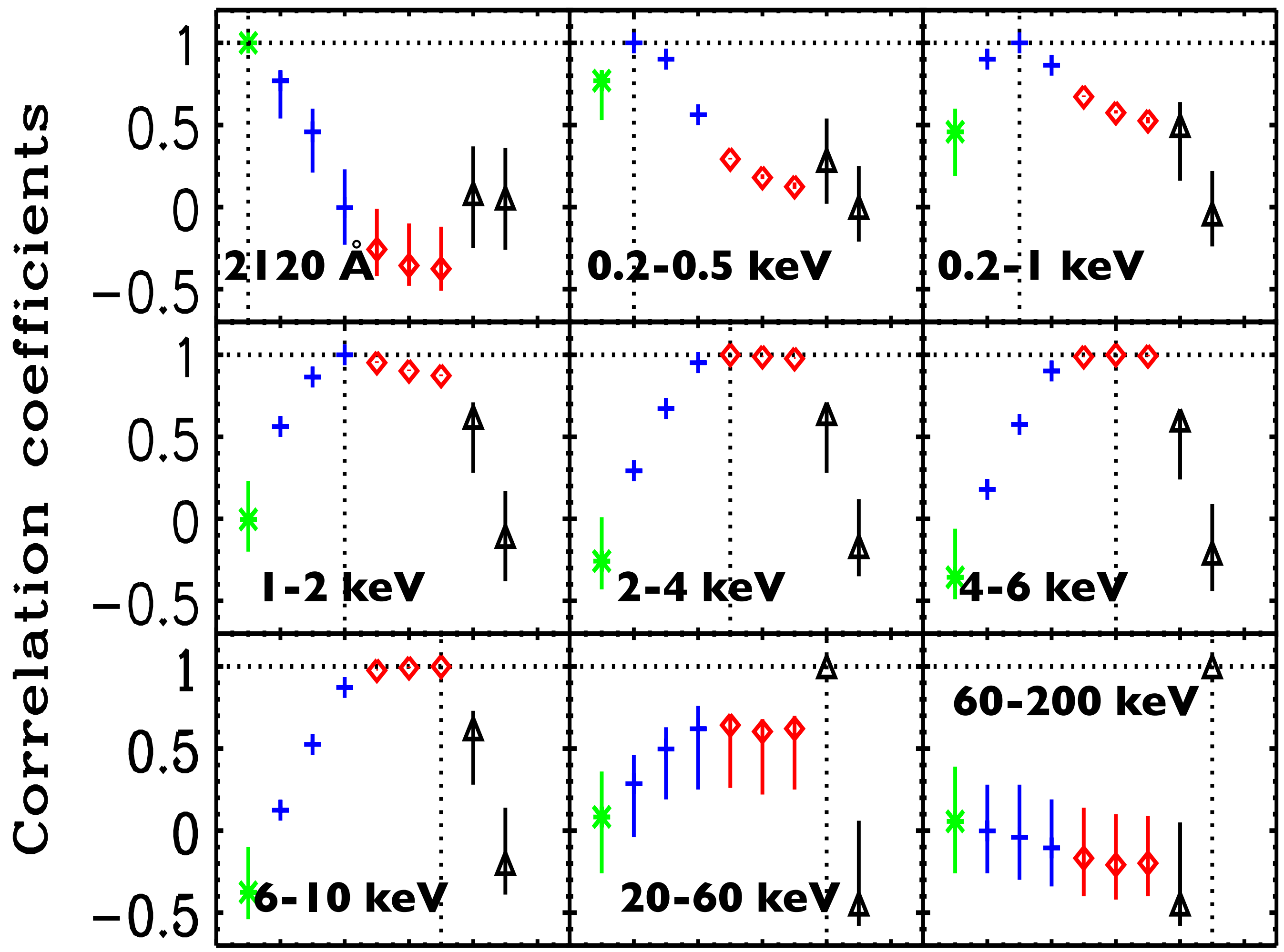

Light curves

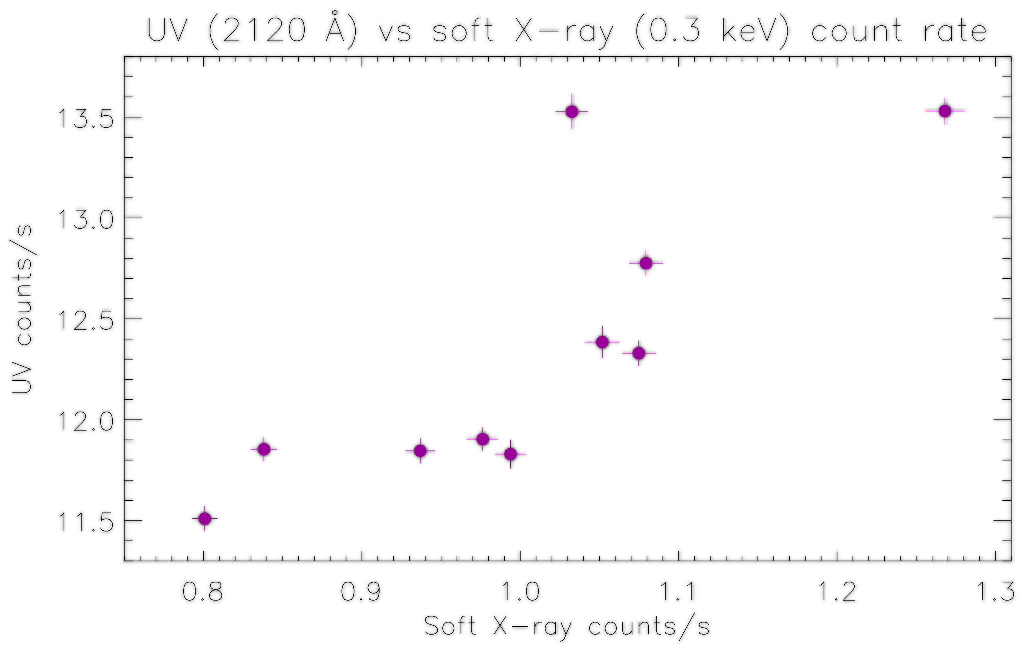

- UV and Soft X are correlated
- UV-Soft X and hard X vary independently

Principal Component Analysis

PCA transform a number of (possibly) correlated variables into a (smaller) number of uncorrelated variables called principal components.

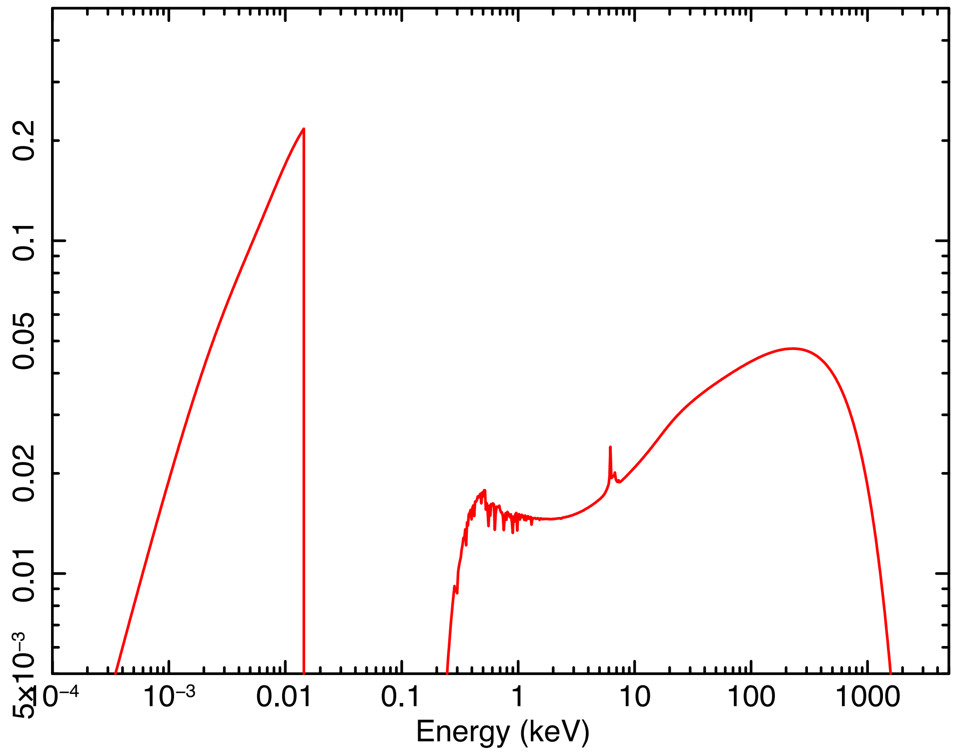

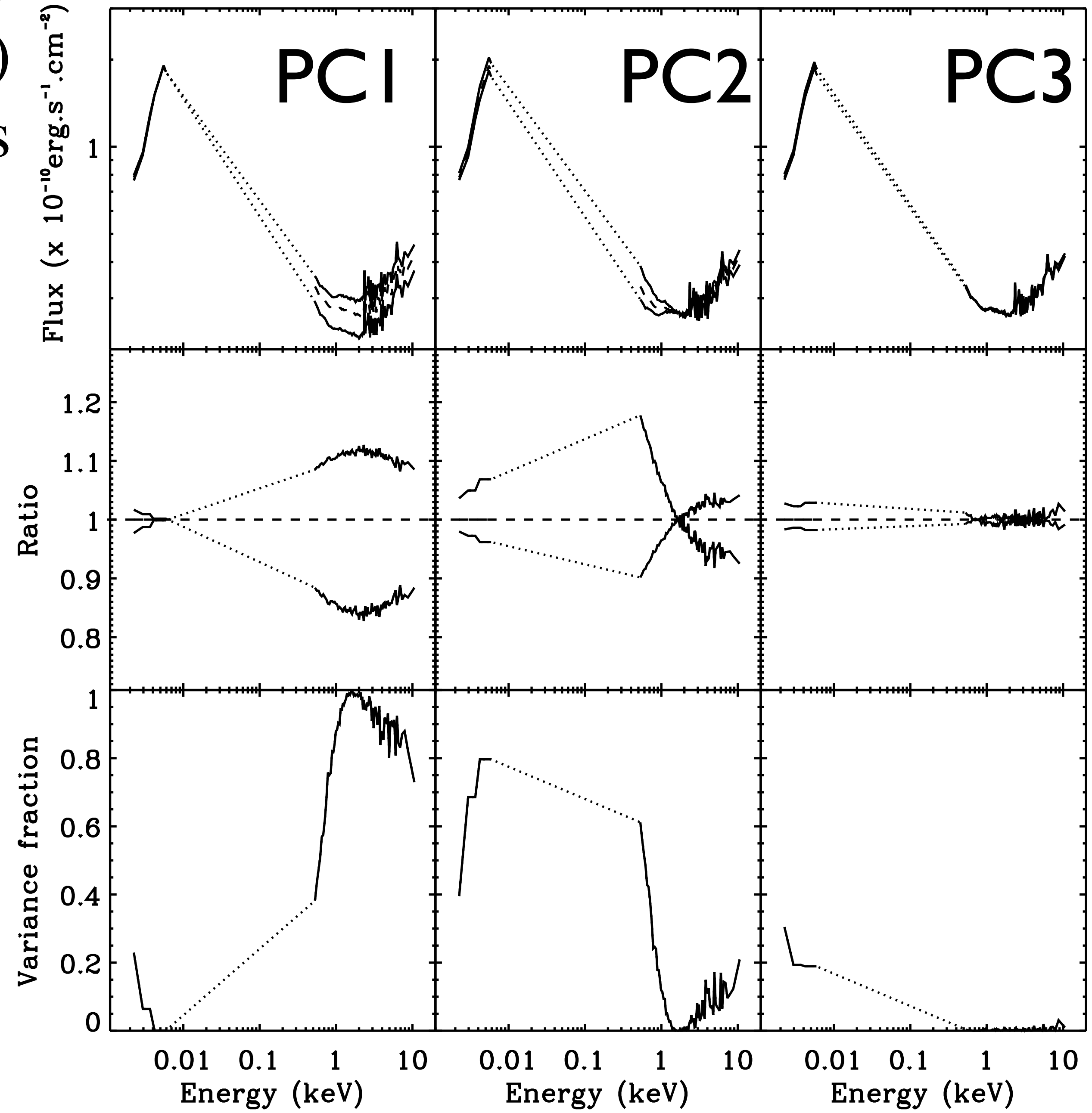

In agreement with two independent spectral components

Principal Component Analysis

PCA transform a number of (possibly) correlated variables into a (smaller) number of uncorrelated variables called principal components.

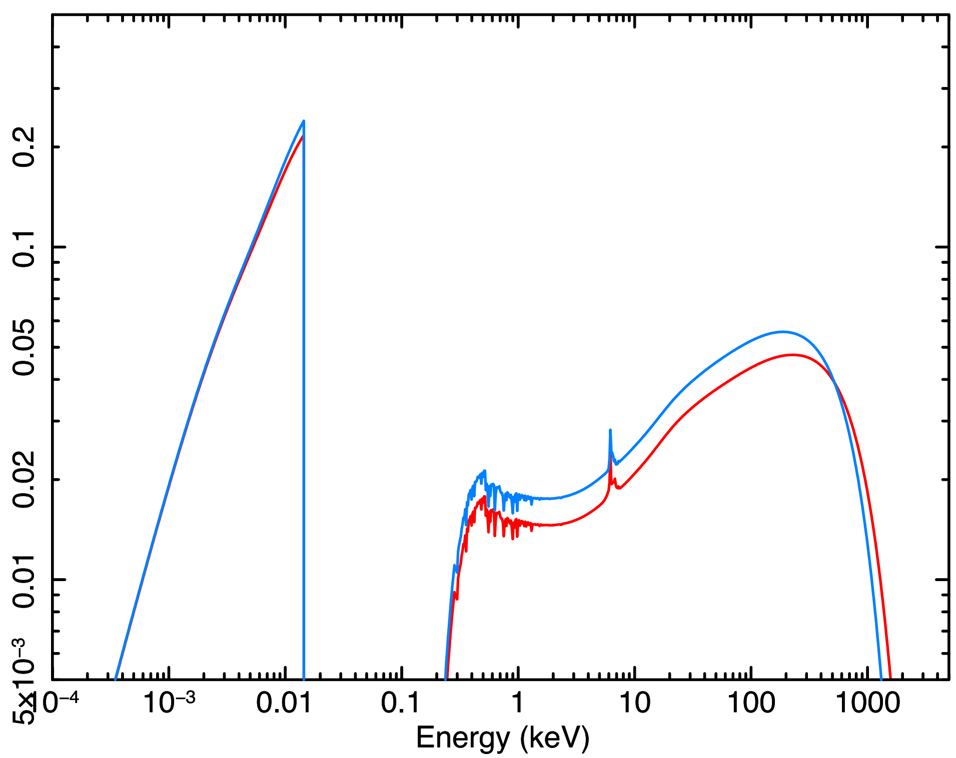

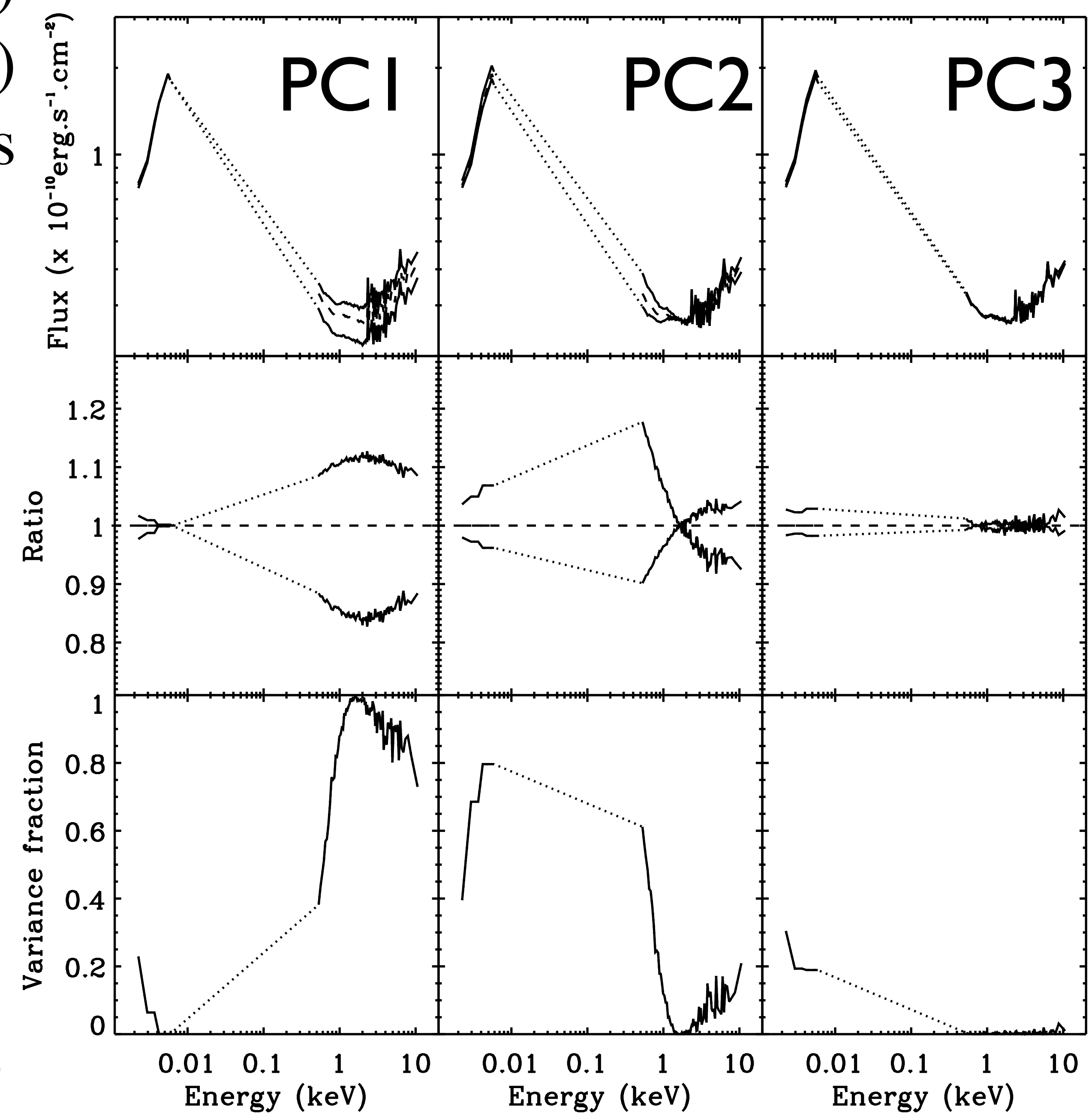

In agreement with two independent spectral components

Reflecting material

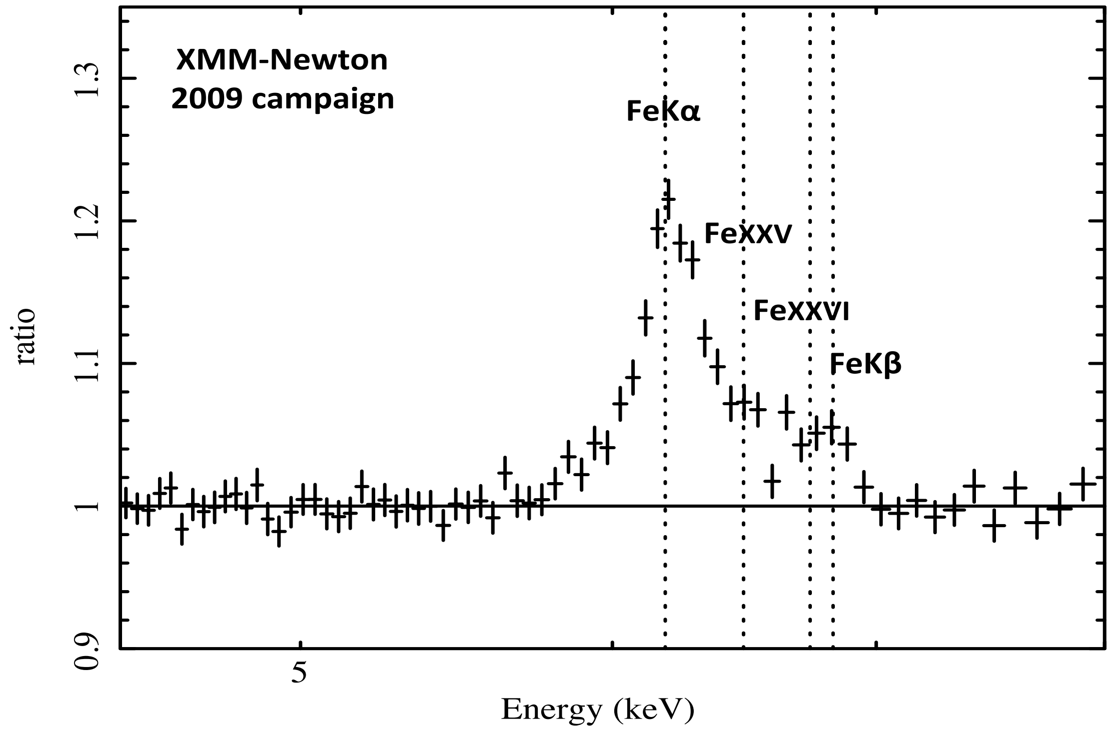

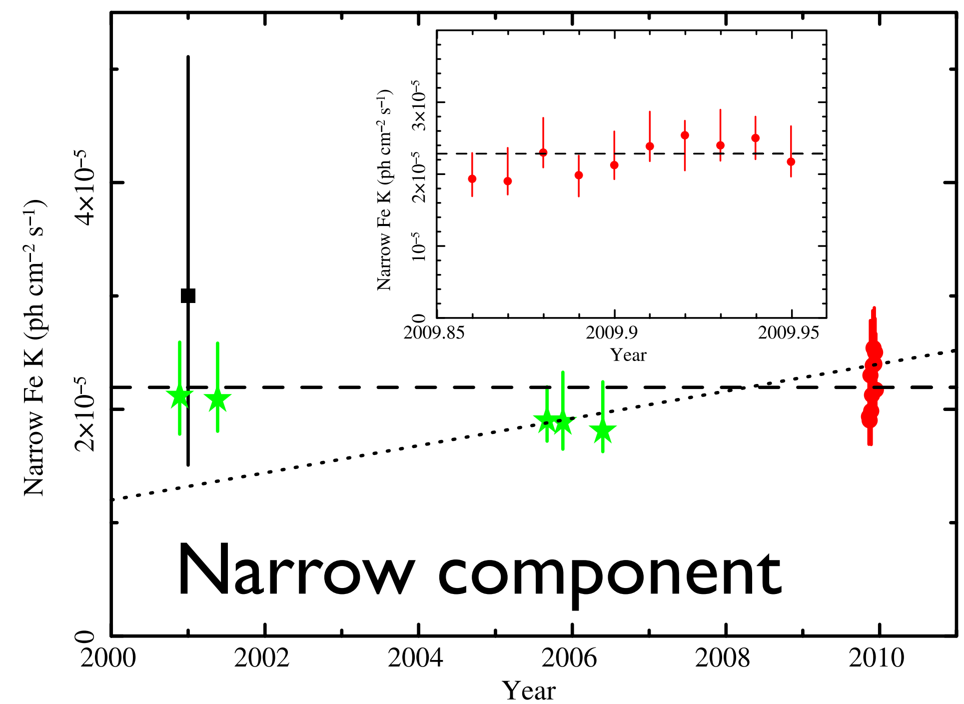

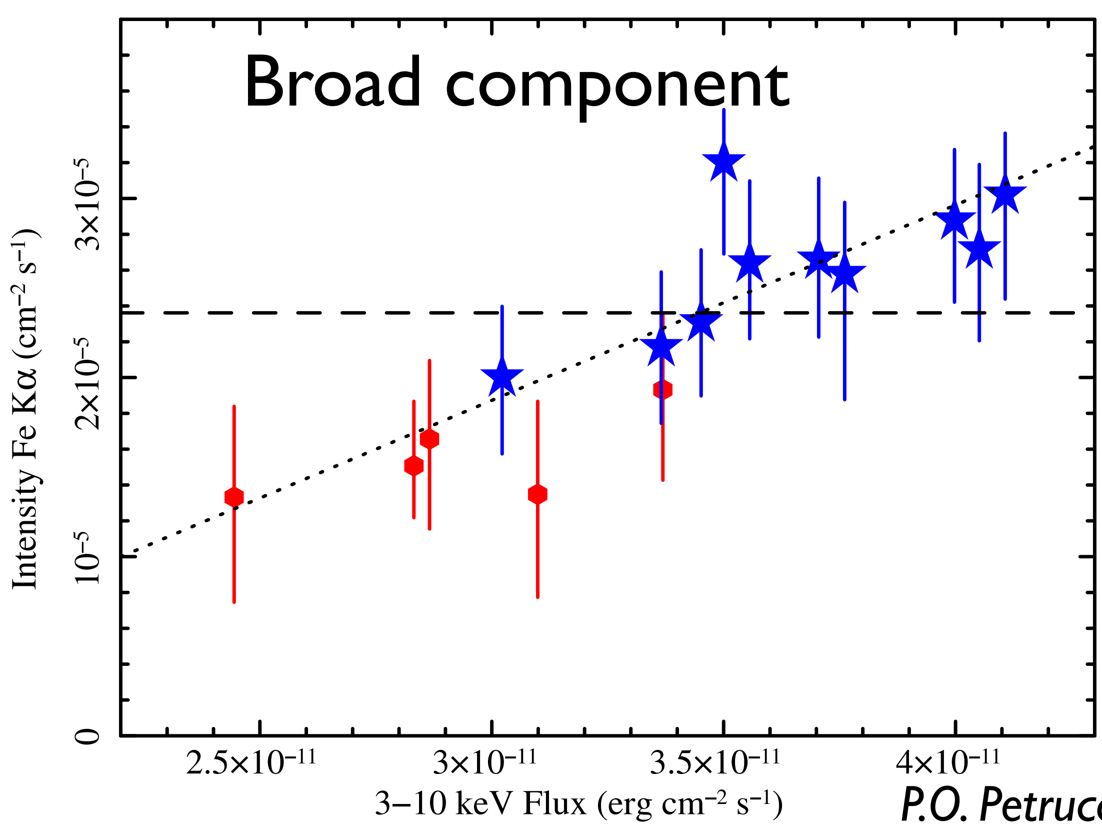

- The iron line profile is composed by a narrow and a broad (non relativistic) component.
- The narrow component is constant.
  - ➜ Remote reflection
- The broad component correlates with the continuum on a few days time scale
  - ➜ outer part of the disc, BLR

The Model

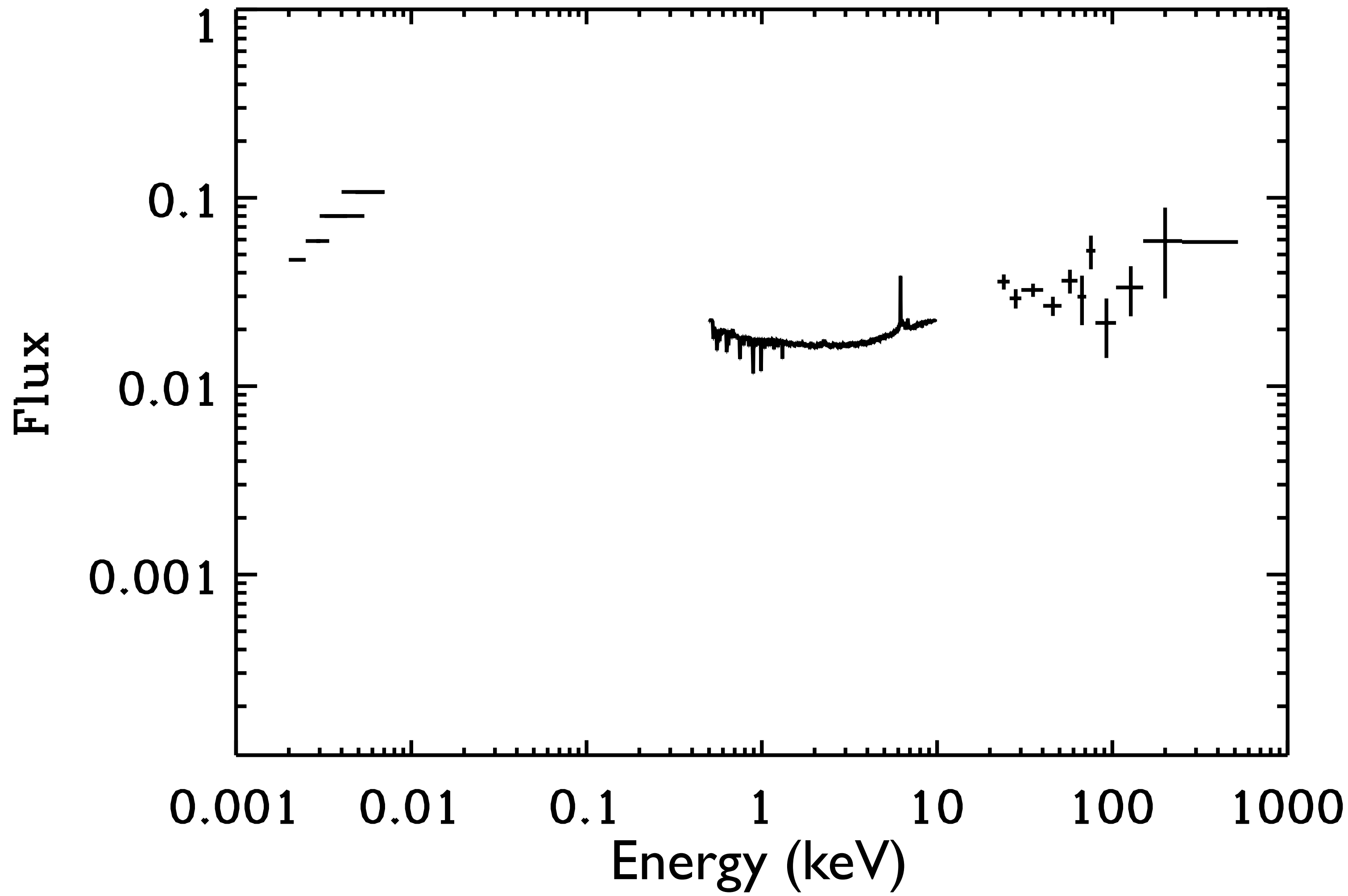

The Model

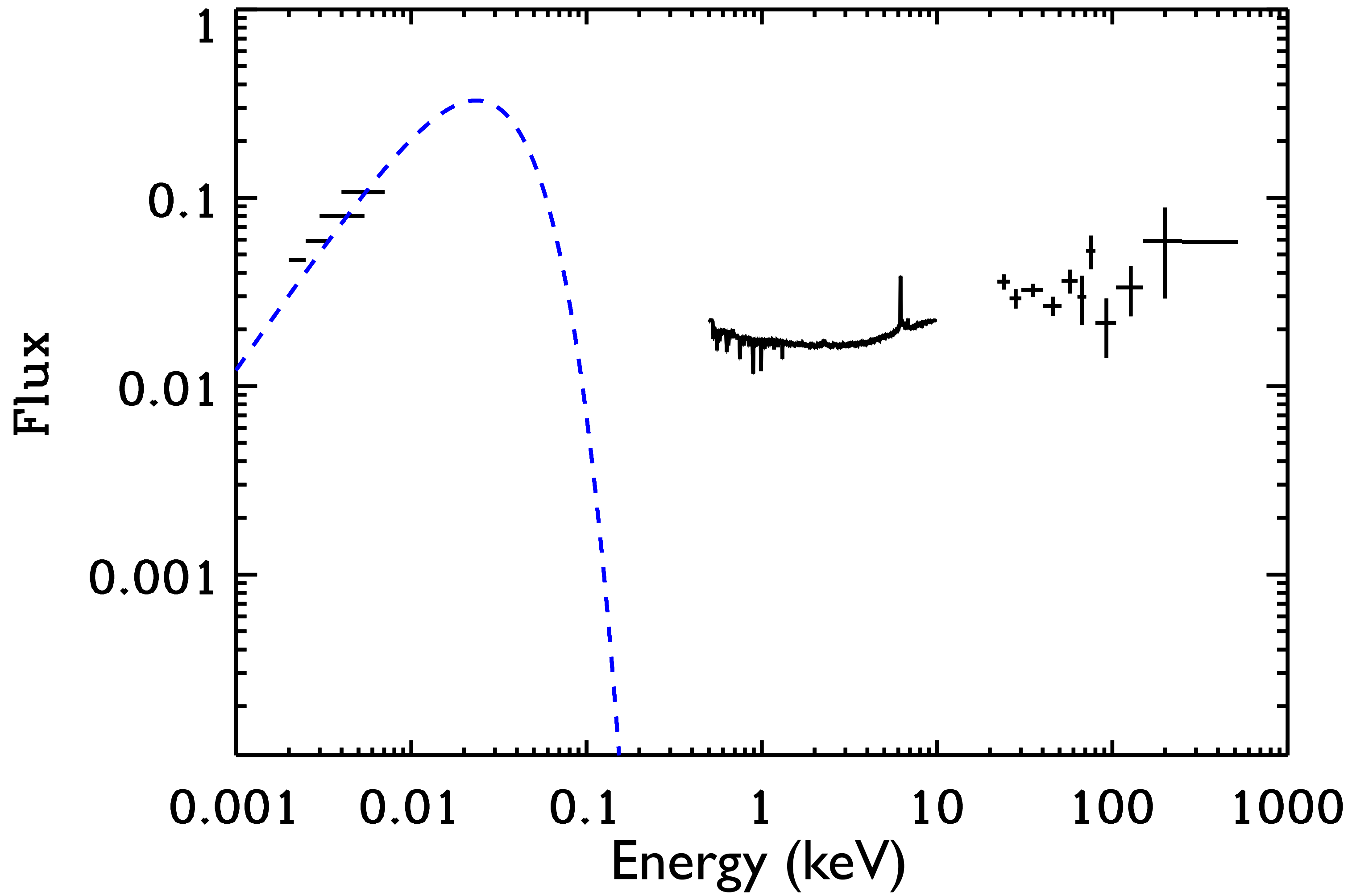

- A multi-black body disc to fit the optical-UV data

The Model

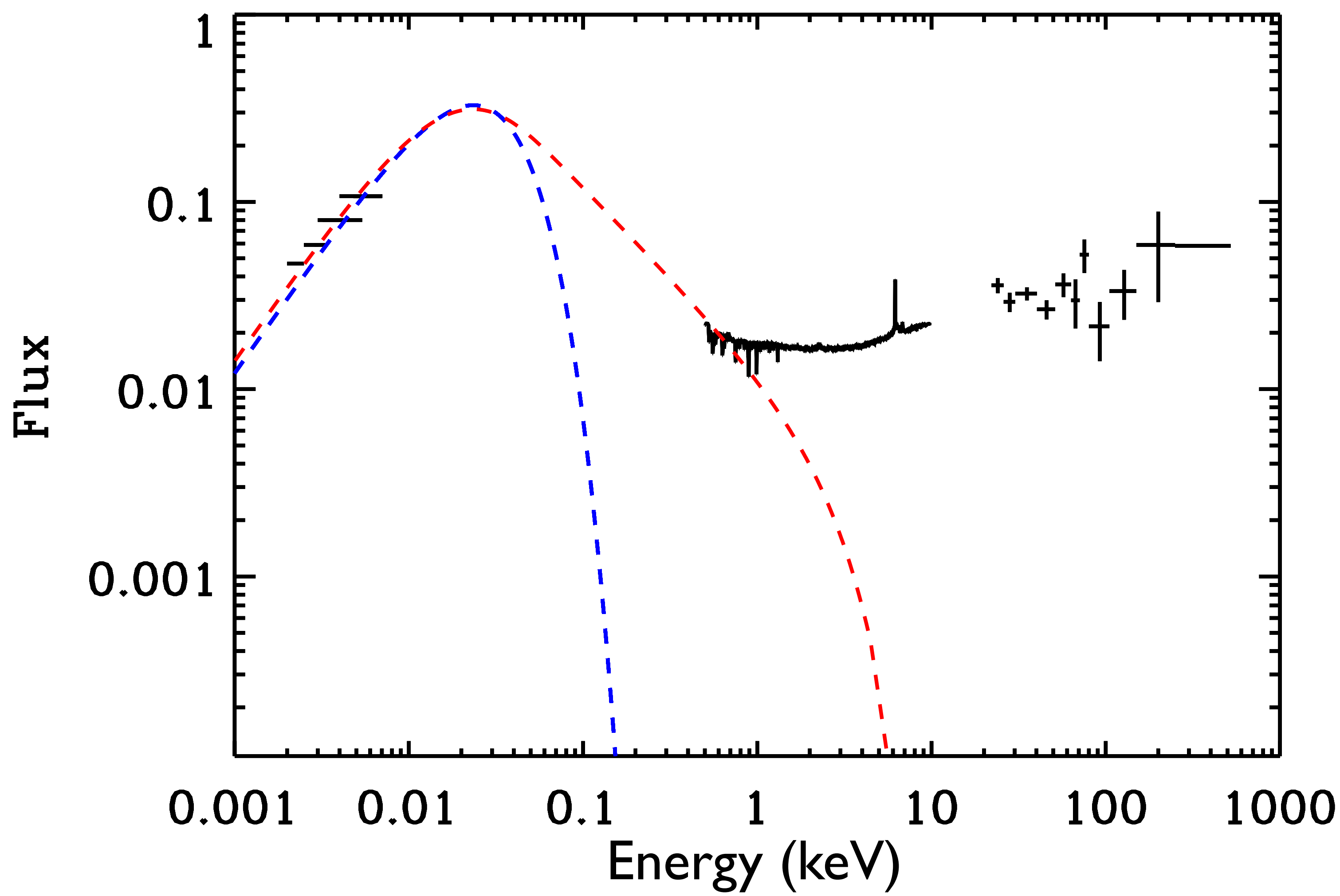

- A multi-black body disc to fit the optical-UV data
- A "warm" corona to fit the soft X-ray emission

The Model

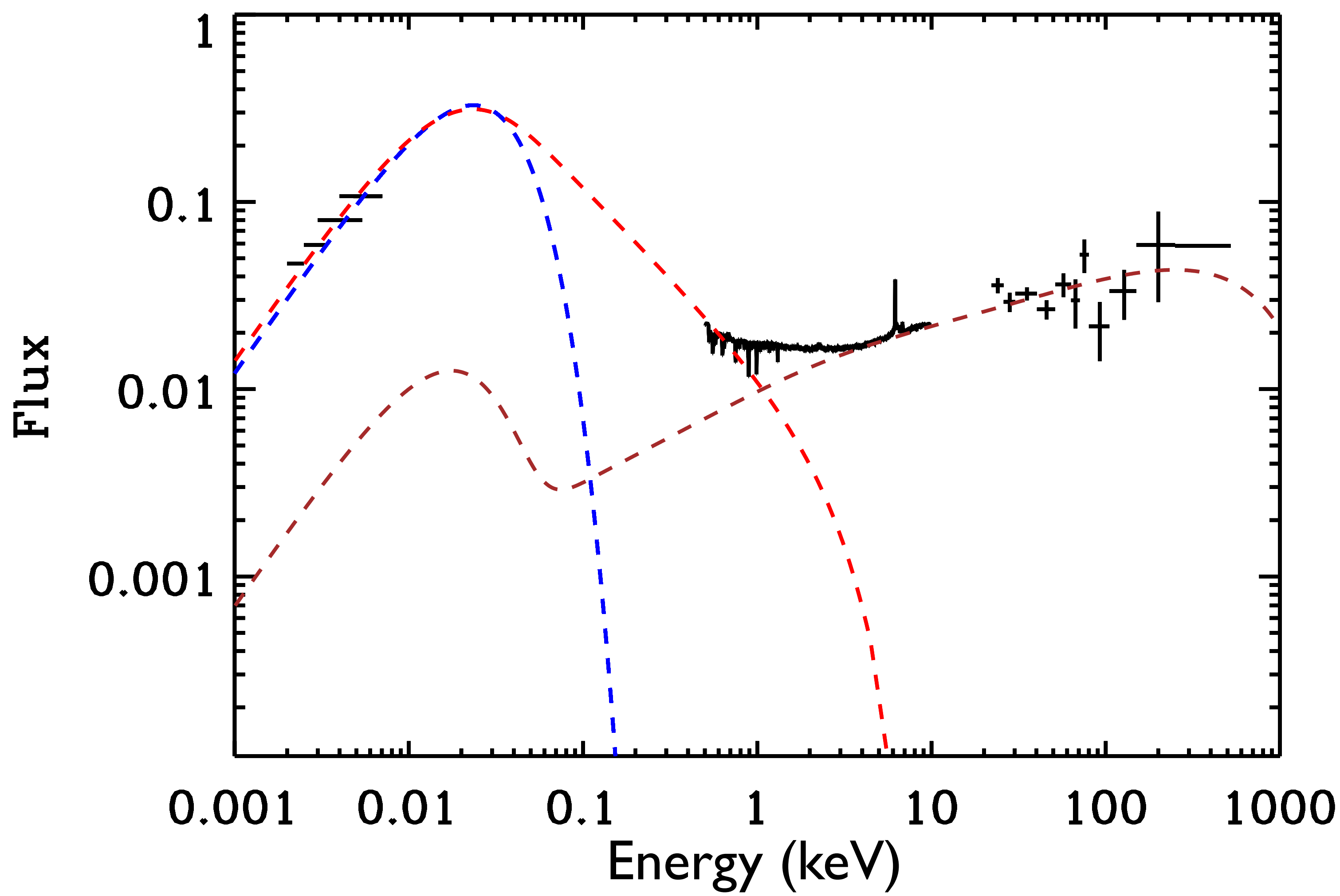

- A multi-black body disc to fit the optical-UV data
- A “warm” corona to fit the soft X-ray emission
- A “hot” corona to fit the hard X-rays

The Model

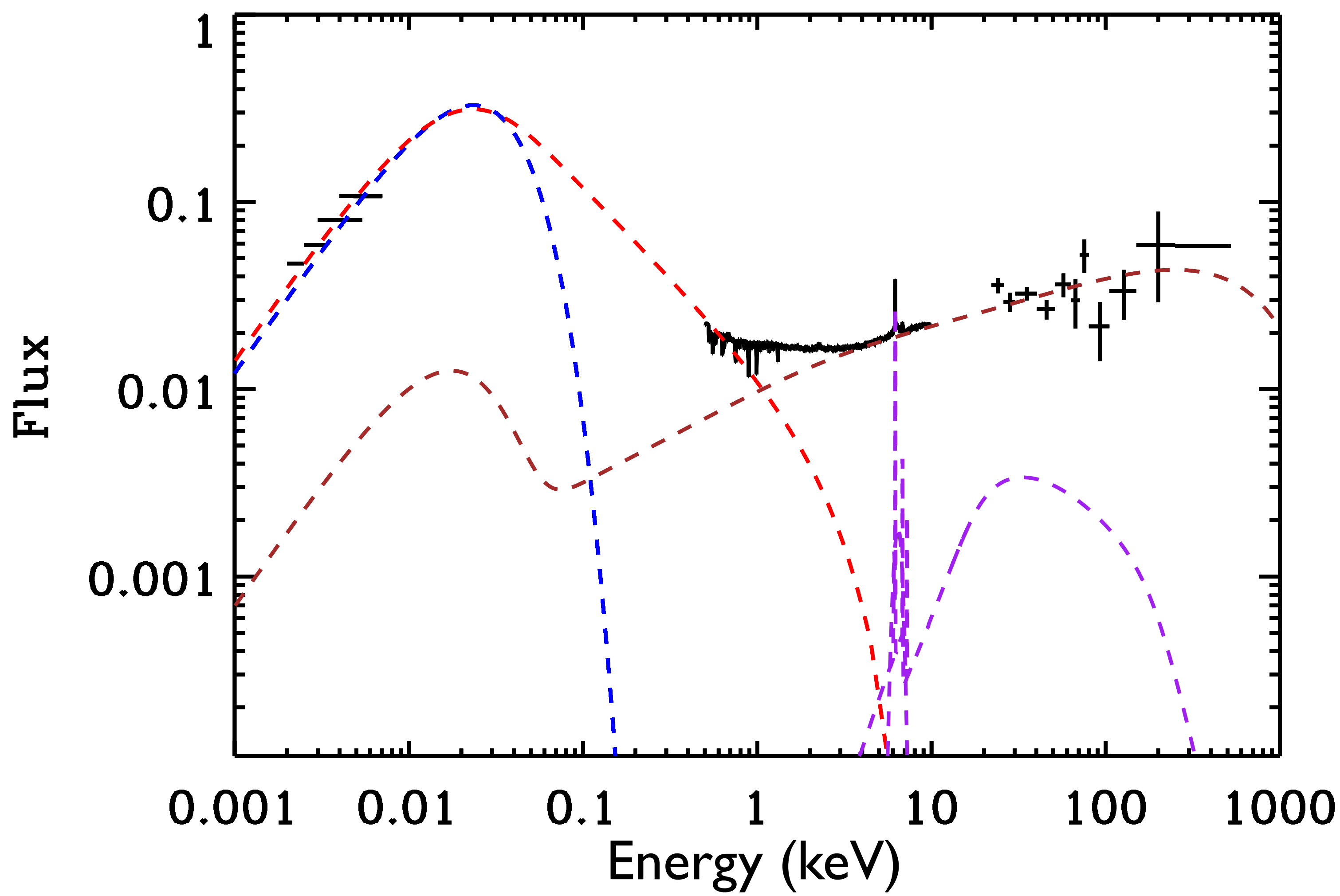

- A multi-black body disc to fit the optical-UV data
- A “warm” corona to fit the soft X-ray emission
- A “hot” corona to fit the hard X-rays
- Reflection components to fit the iron line profile

The Model

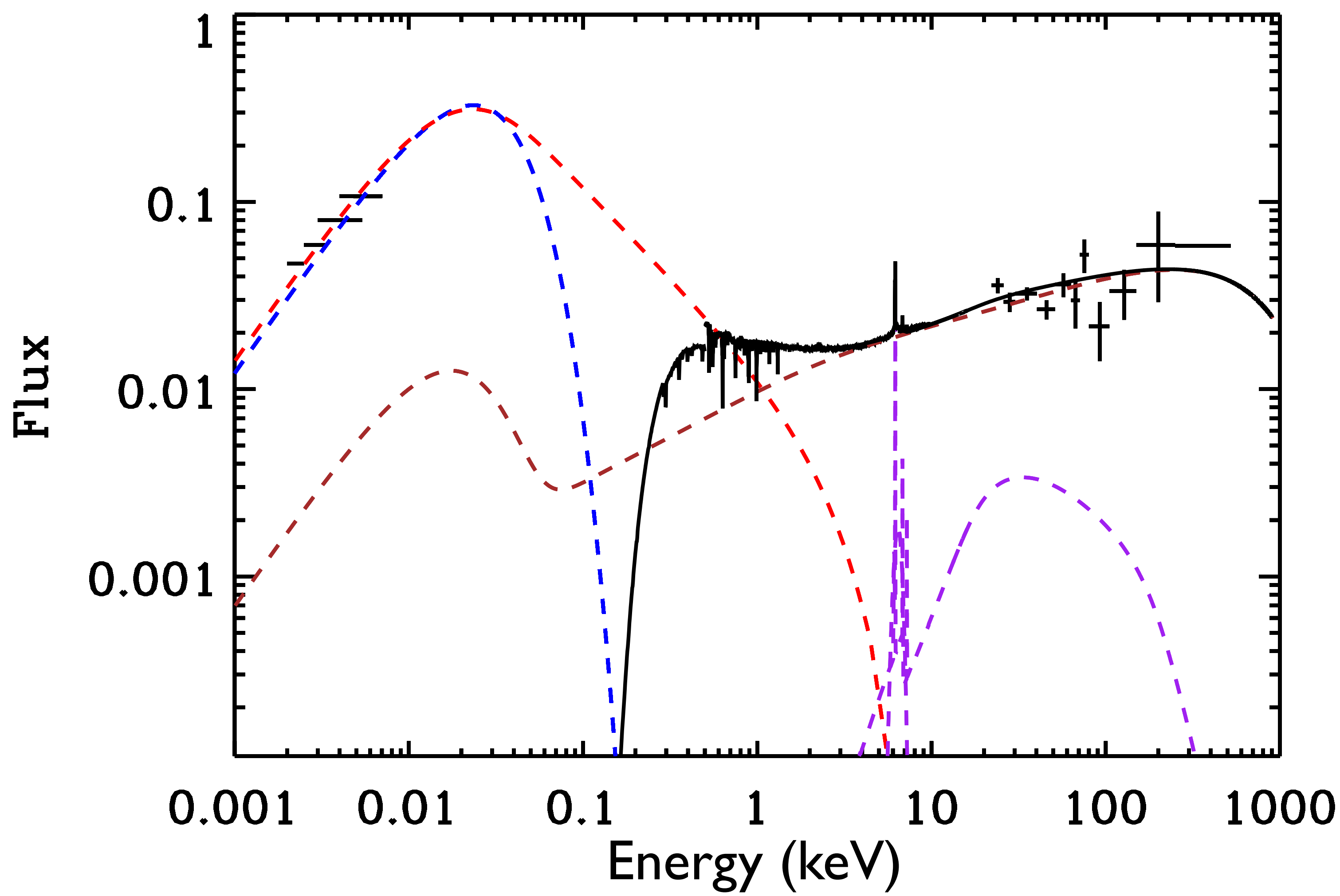

- A multi-black body disc to fit the optical-UV data
- A "warm" corona to fit the soft X-ray emission
- A "hot" corona to fit the hard X-rays
- Reflection components to fit the iron line profile
- A warm absorber from the outflow analysis

Best Fit Model Parameters

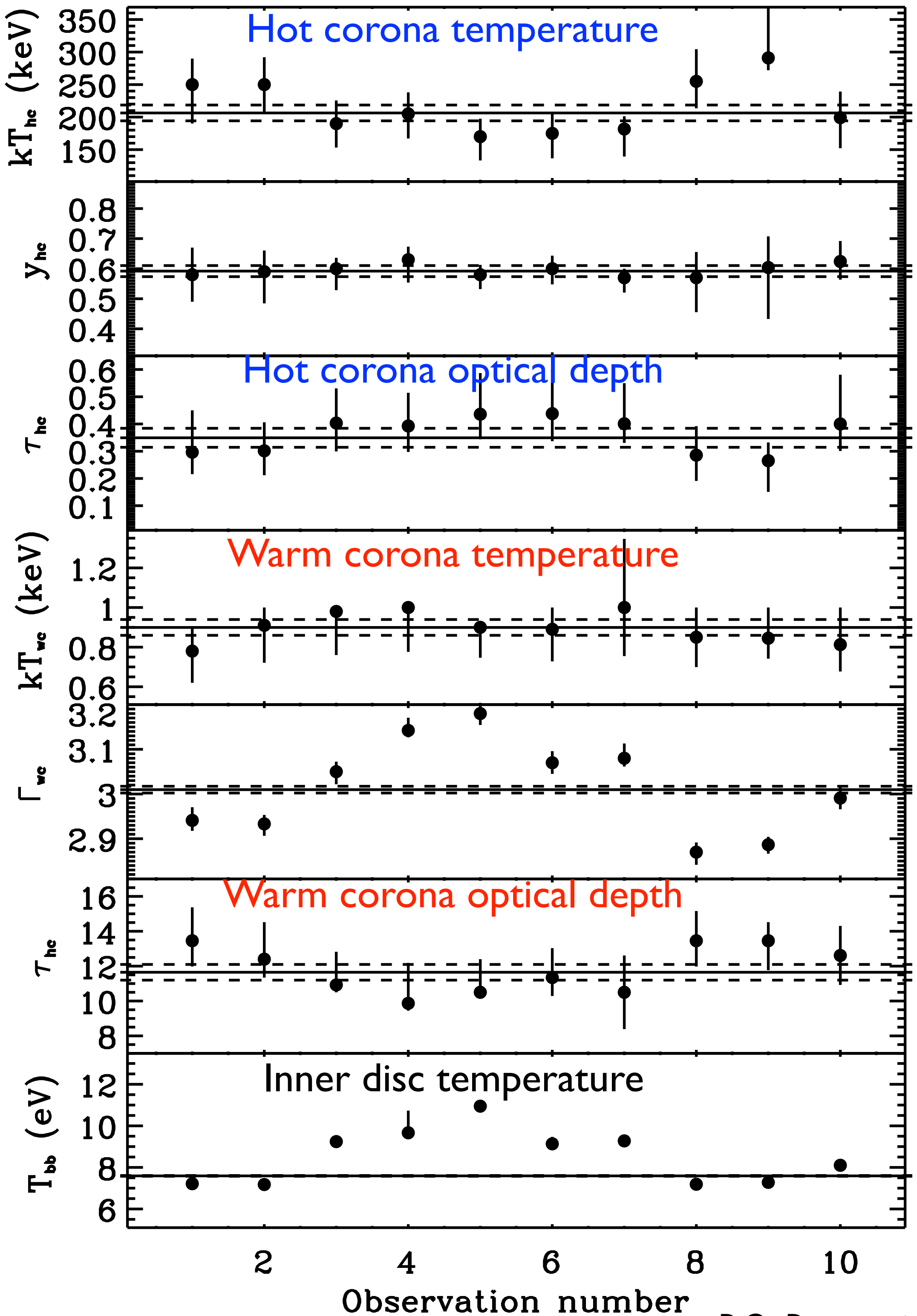

- Hot corona temperature~200 keV and optical depth~0.35

- Warm corona temperature~1 keV and optical depth~10

- $$F_{disc} \simeq \pi R_{in}^2 \sigma T_{in}^4$$

The disc flux agrees with the presence of the disc down to a few R_{Sch}

Hot vs Warm coronae

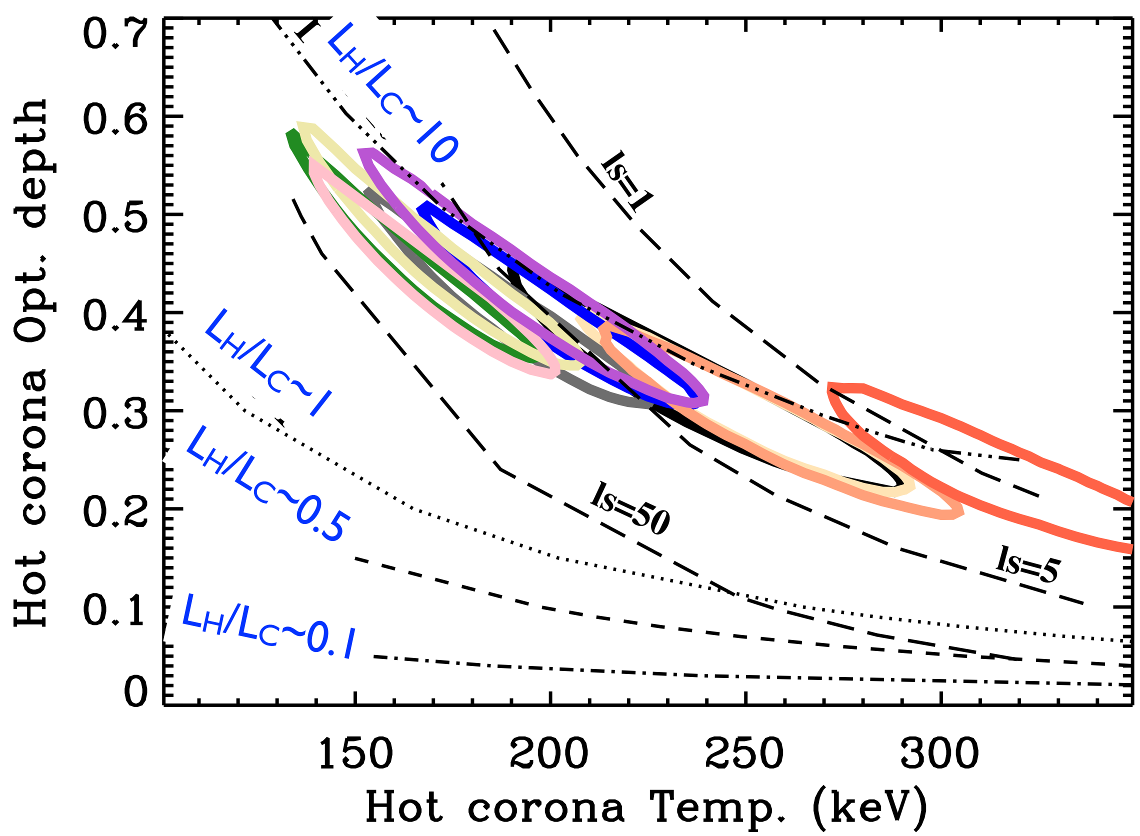

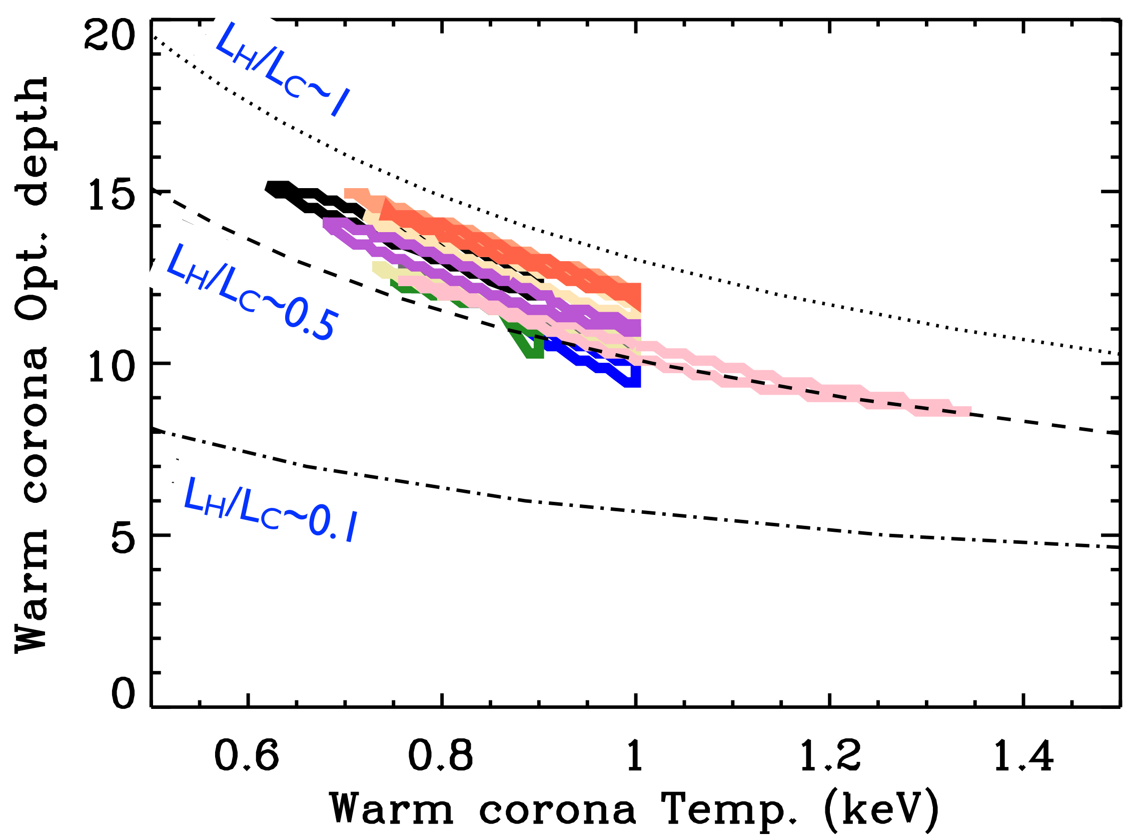

$L_H/L_C \sim 10$

$L_H/L_C < 1$

➡ Photon starved geometry

➡ (Slightly) photon fed geometry

Origin of the variability

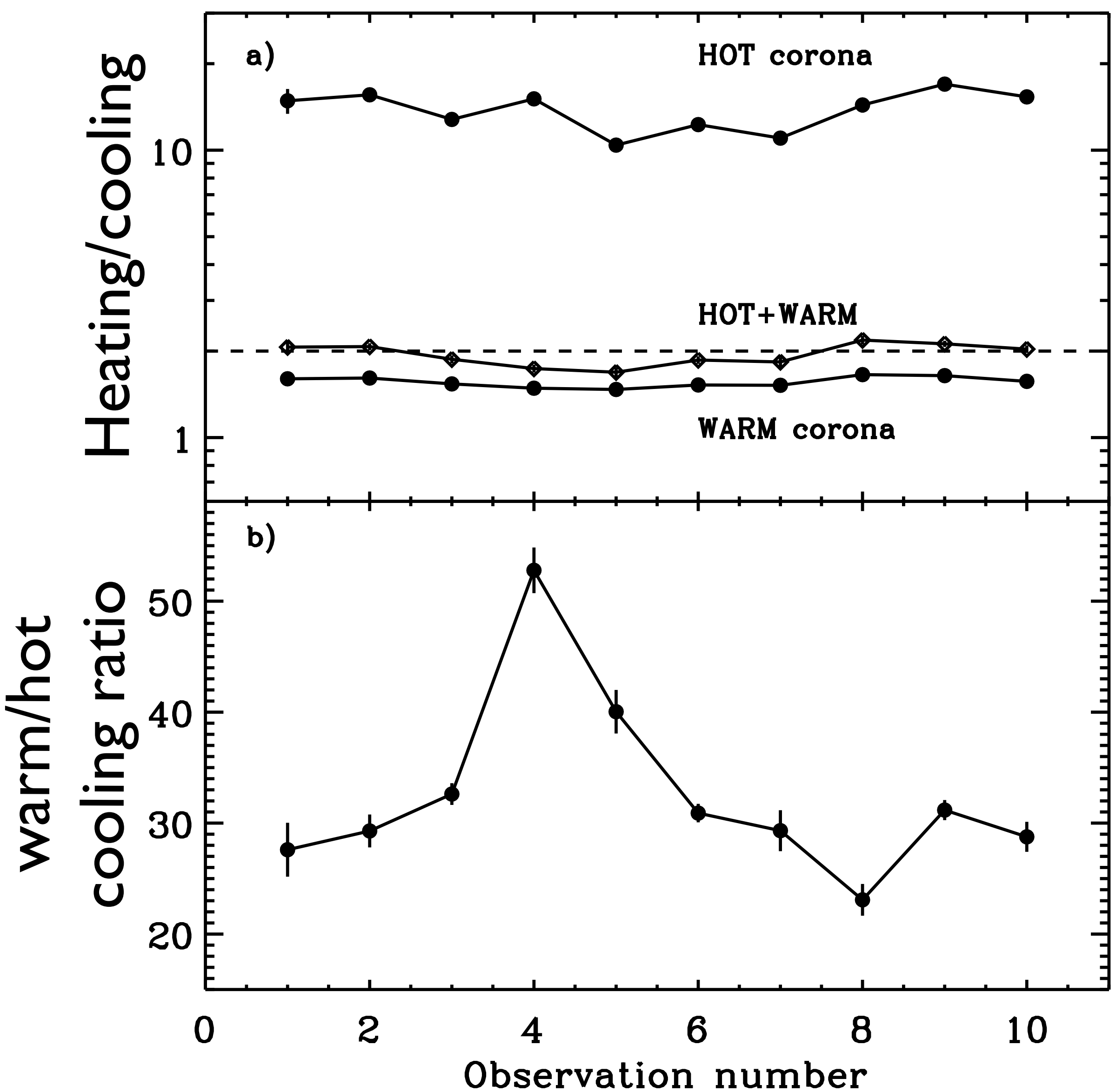

•L_H/L_C varies

→ disc/corona configuration varies

•The disc UV emission varies by tens of % while the corona cooling varies by large factor

→ variation of the geometry (especially of the hot corona)

A Possible Geometry

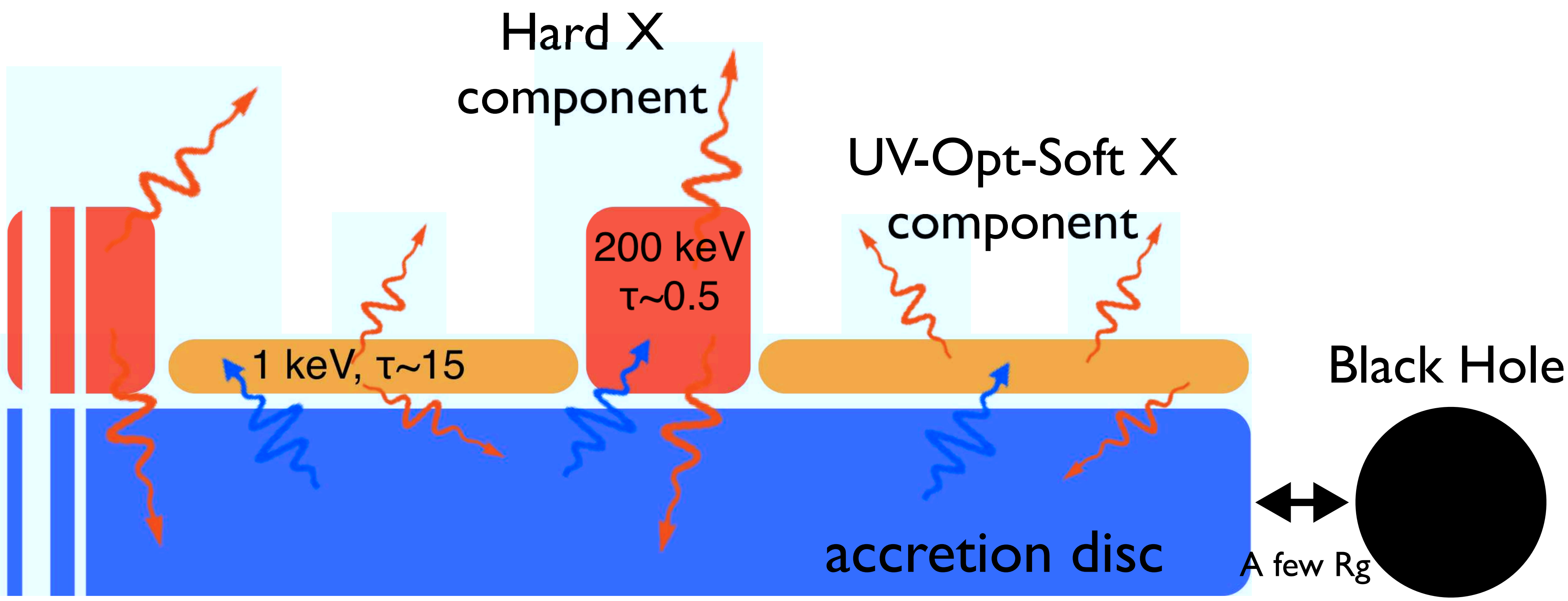

The Outflow of Mkn 509

Stacked RGS spectrum

- Total exposure: 600 ks
- Several narrow absorption lines
- Detection 31 individual ions
- Tight upper limits column densities other 18 ions
- Two main velocity components (-10 and -300 km/s)
- Highly ionised ions in general higher velocity

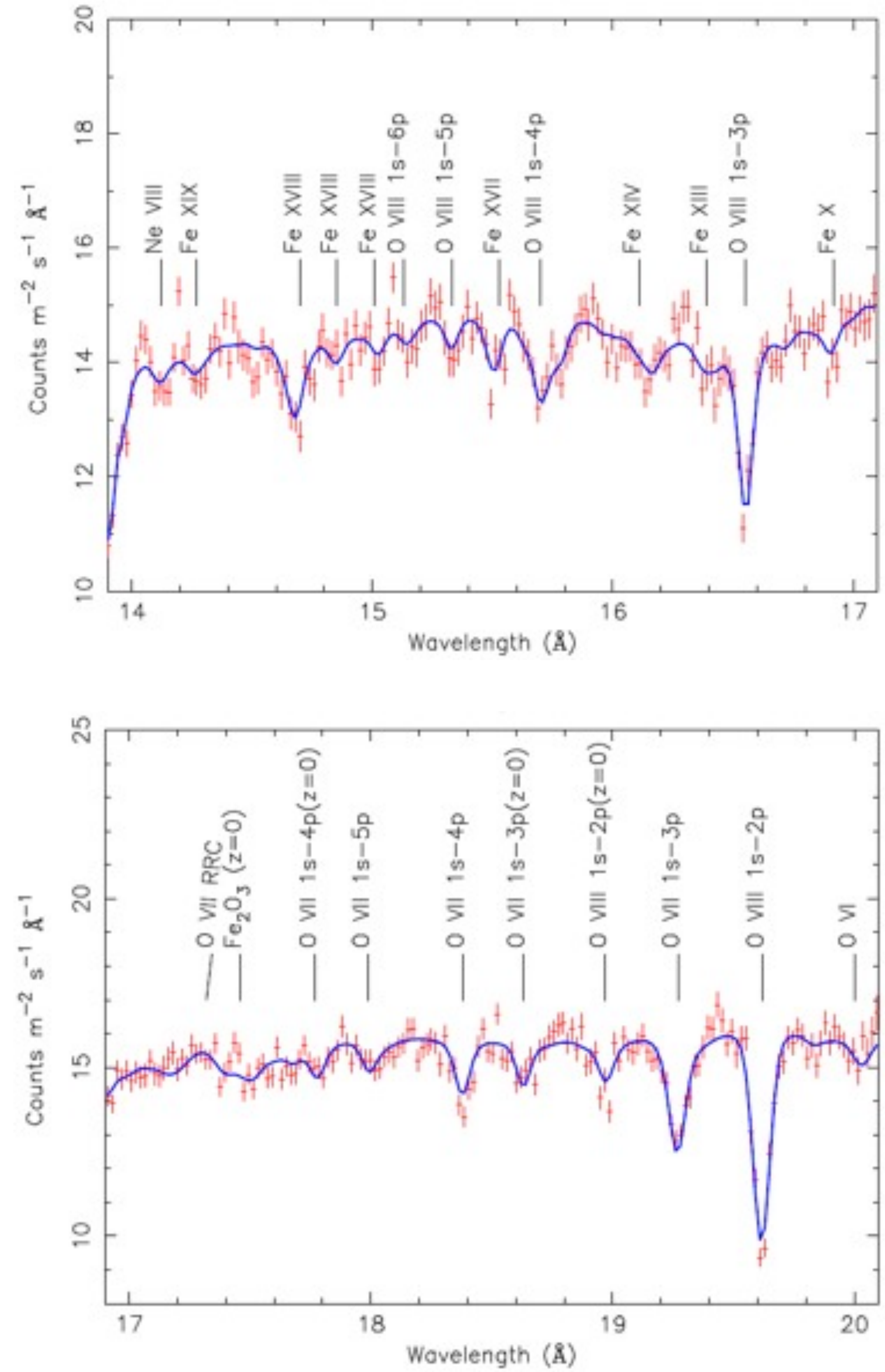

Discrete versus continuous absorption measure distribution?

- Column densities well approximated by sum of 5 components

Component	$\log \xi^a$	N_H^b
A	-0.26 ± 0.55	0.26 ± 0.12
B	0.73 ± 0.16	0.84 ± 0.10
C	2.08 ± 0.03	4.8 ± 0.4
D	2.84 ± 0.06	5.7 ± 0.9
E	3.55 ± 0.25	49 ± 85

[a] Ionization parameter in 10^{-9} W m.
[b] Column density in units of 10^{24} m^{-2}.

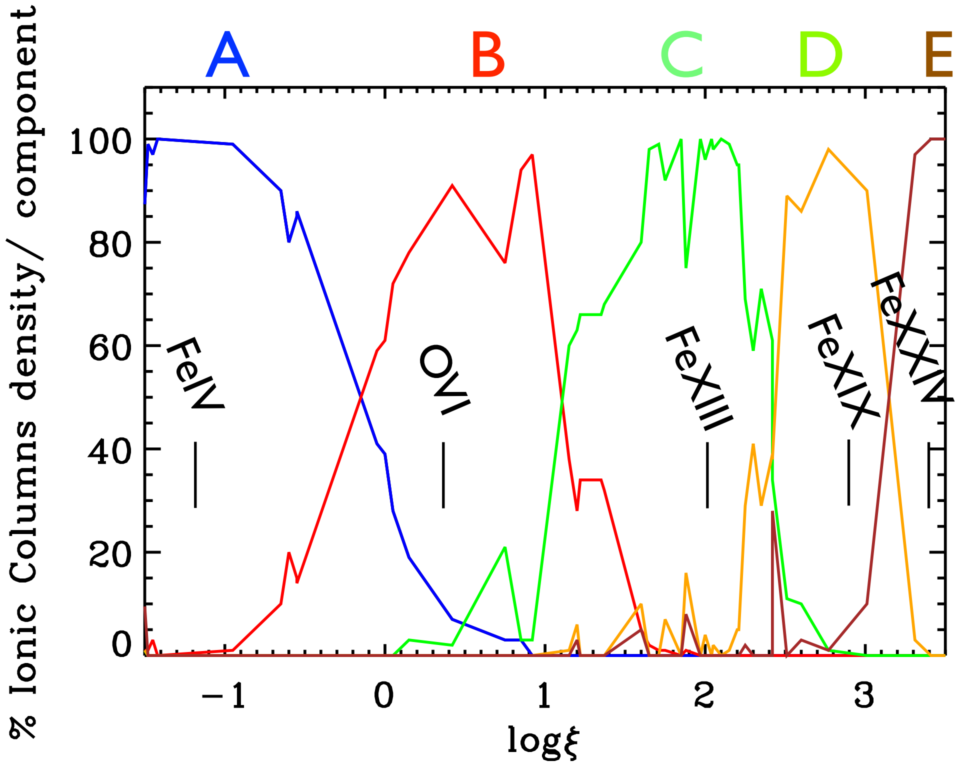

- Higher column for higher ionisation parameter

➡ density stratification

Abundances, Velocities

		(solar)
C/O	1.19±0.08	(0.97)
N/O	0.98±0.08	(0.90)
Ne/O	1.11±0.10	(0.91)
Mg/O	0.68±0.16	(0.87)
Si/O (LETGS)	1.3±0.6	(0.87)
S/O	0.57±0.14	(0.83)
Ca/O	0.89±0.25	(0.73)
Fe/O	0.85±0.06	(0.86)

Steenbrugge et al. (2011)

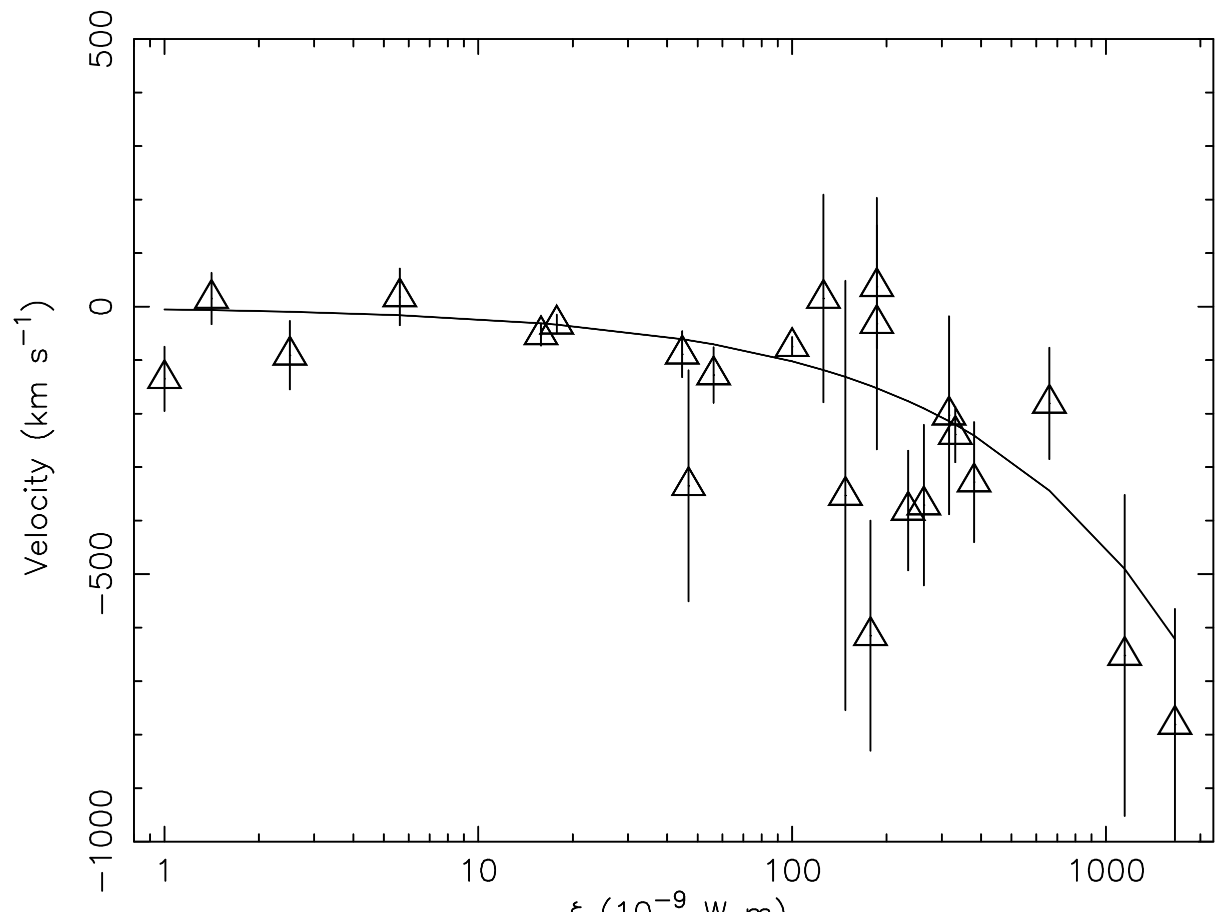

Dermer et al. (2011)

IPAG
Institut de Planétologie et d'Astrophysique de Grenoble

Where is the gaz?

- Needs time-dependent model
- For each of the 5 components: if L increases, ξ must increase (as $\xi = L/nr^2$)

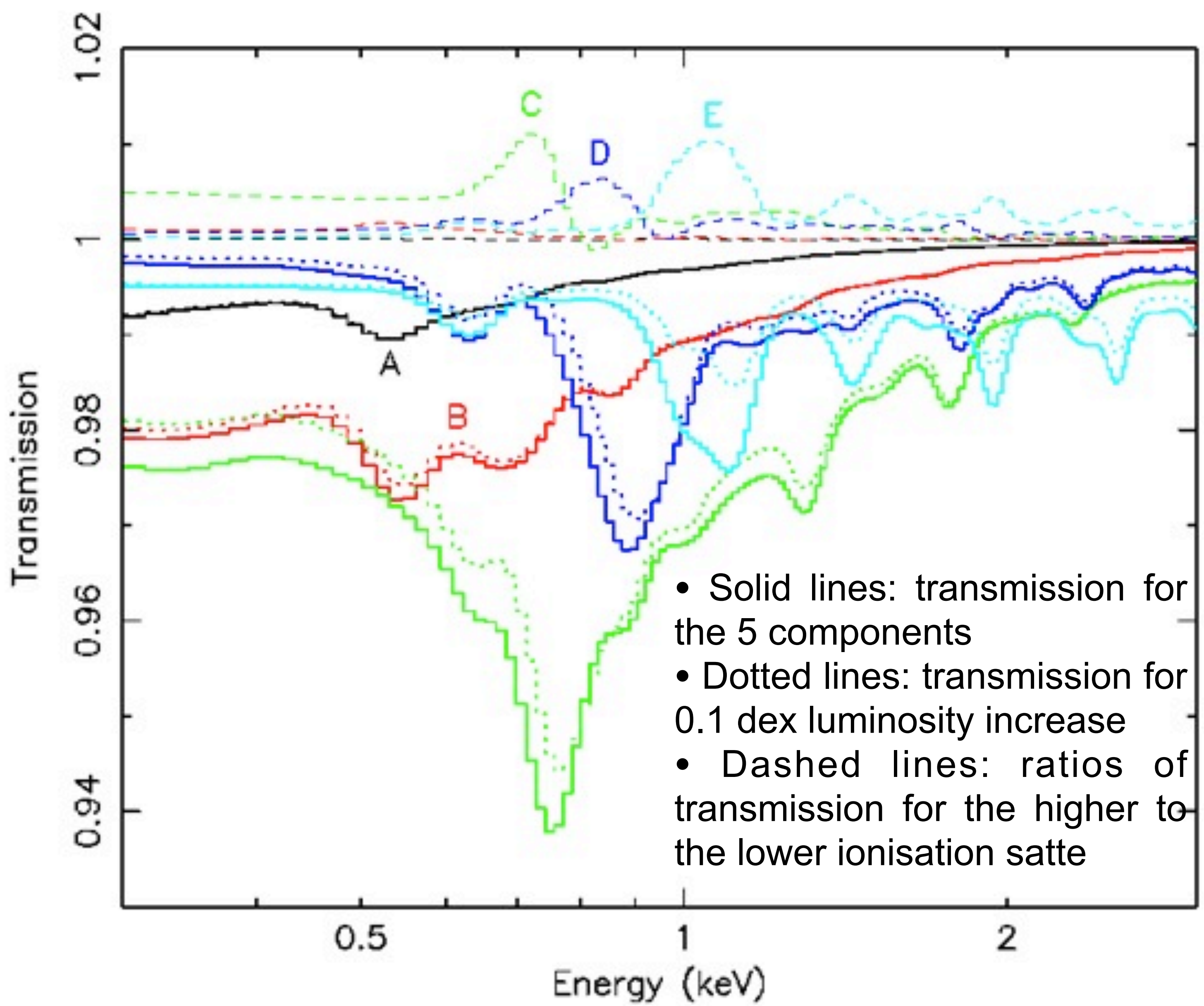

IPAG
Institut de Planétologie
et d'Astrophysique
de Grenoble

Where is the gaz?

- From 10 continuum model fits

➔ predicted ξ change for each of 10 observations, compared to average spectrum

- If gas responds immediately, transmission outflow changes immediately

- Changing the distance *r* of the gas to the central source will change the time delay and the gas density (nr^2=L/ξ=cste) i.e. the ionisation/recombination times.

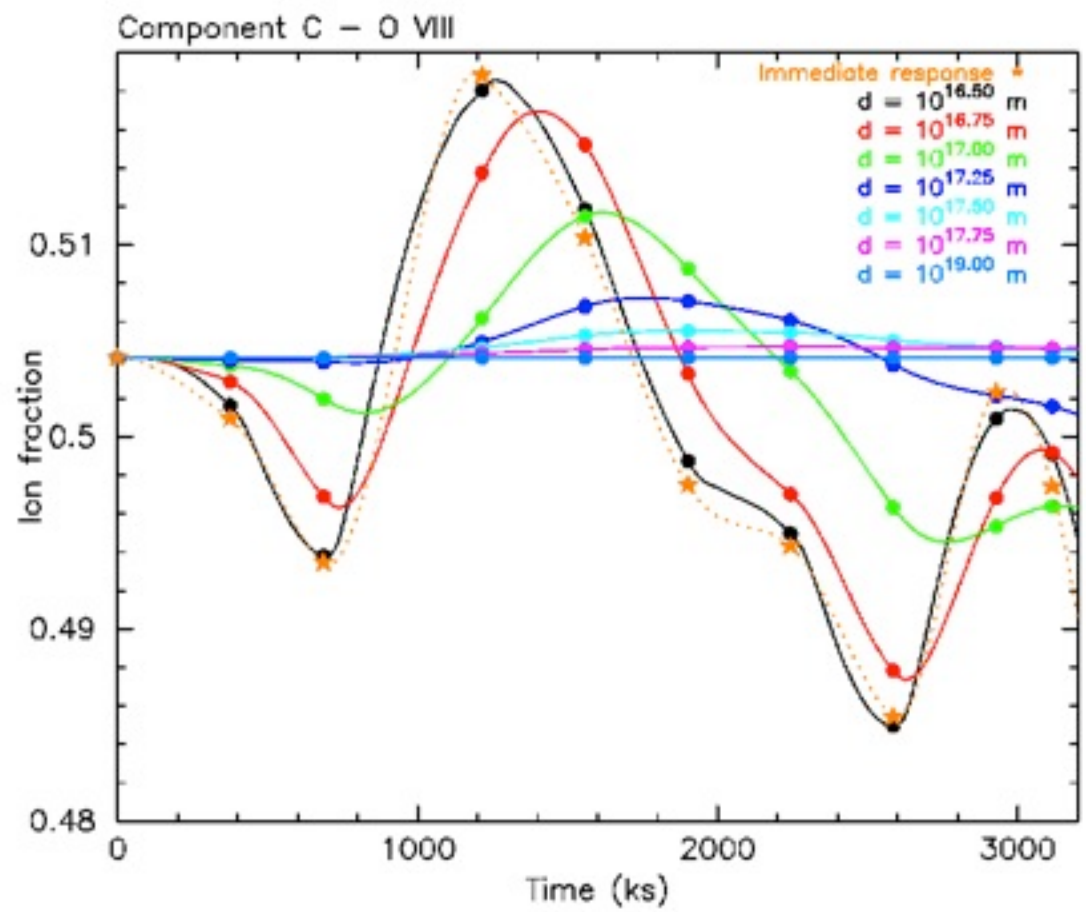

Component	Distance (pc)
C	>91
D	>5.8
E	>5.4

Kaastra et al. (2011b)

Mass loss through the wind

$$\dot{M}_{loss} = \Omega m_p n r^2 v \qquad n r^2 \cdot v = (L/\xi)\cdot v$$

$$\dot{M}_{loss} < \dot{M}_{acc} \qquad L = \eta \dot{M}_{acc} c^2$$

$$\boxed{\Omega < \frac{(\xi / v)}{\eta m_p c^2}}$$

v (km/s)	-100	-1000
ξ=1	0.001	0.0001
ξ=1000	1.0	0.1

Outflows in Mkn 509

- Originate at a few pc (from the torus?)
- Higher column for higher ionisation parameter
- Higher outflow velocity for higher ionisation parameter
- It should occur in narrow, density stratified streamers

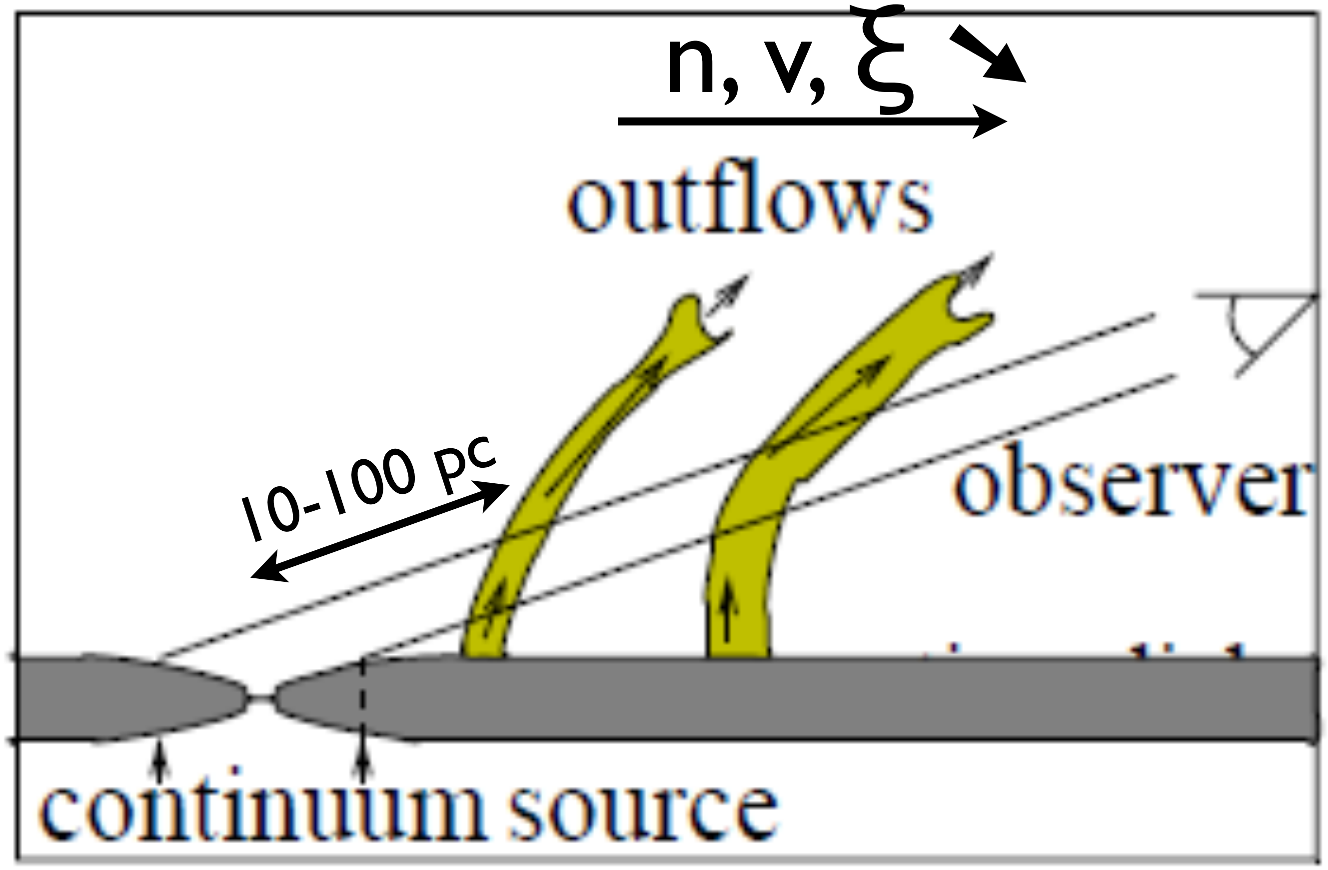

The Big Picture

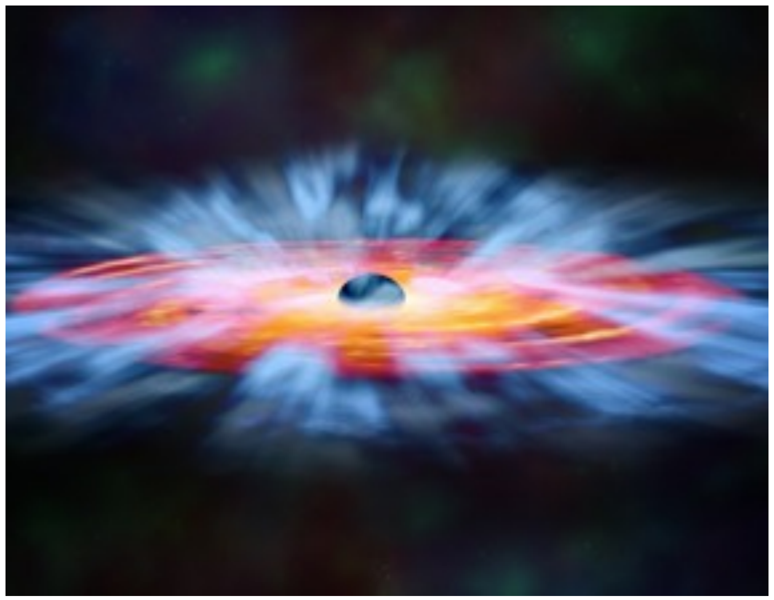

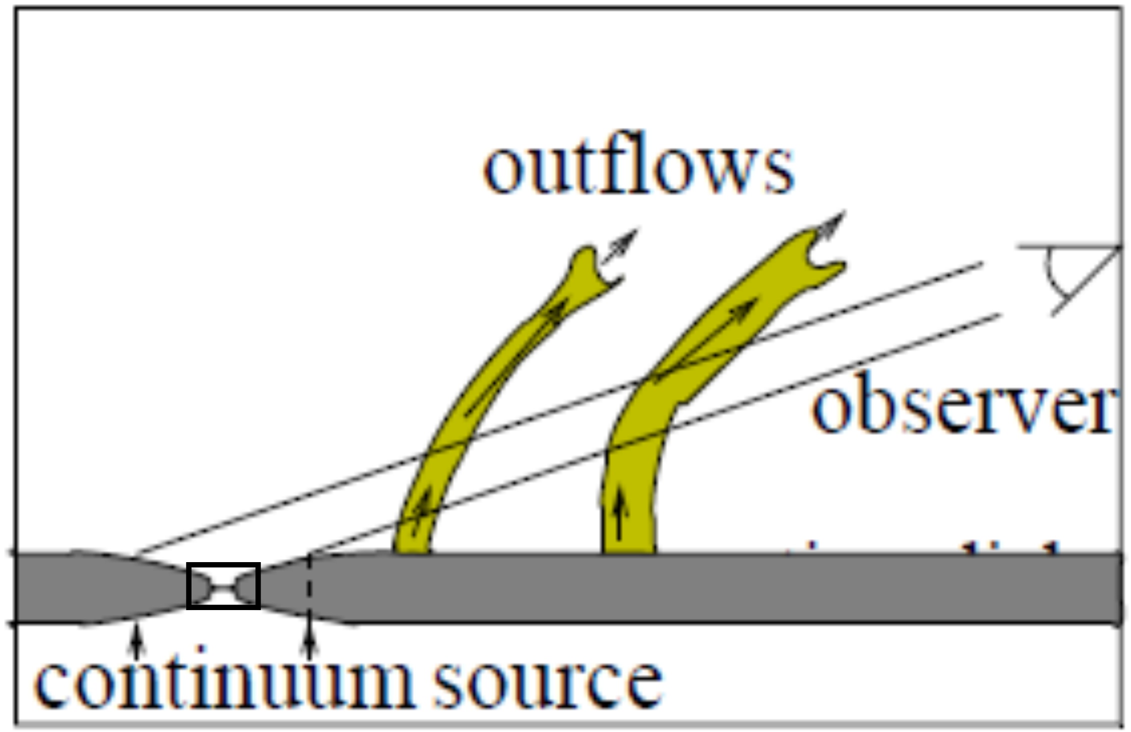

The Big Picture